Chemical Geology 335 (2013) 48–62

Contents lists available at SciVerse ScienceDirect

Chemical Geology

journal homepage: www.elsevier.com/locate/chemgeo

Hydrogeochemistry of seasonal flow regimes in the Chena River, a subarctic watershed draining discontinuous permafrost in interior Alaska (USA)

Thomas A. Douglas [a,*], Joel D. Blum [b], Laodong Guo [c], Katy Keller [b,1], James D. Gleason [b]

[a] U.S. Army Cold Regions Research and Engineering Laboratory, P.O. Box 35170, Fort Wainwright, AK 99703, USA
[b] University of Michigan, Department of Earth and Environmental Sciences, 1100 N. University Avenue, Ann Arbor, MI 48109, USA
[c] University of Wisconsin—Milwaukee, School of Freshwater Sciences, 600 E Greenfield Avenue, Milwaukee, WI 53204, USA

ARTICLE INFO

Article history:
Received 21 April 2012
Received in revised form 17 October 2012
Accepted 26 October 2012
Available online 6 November 2012

Editor: B. Sherwood Lollar

Keywords:
Permafrost biogeochemistry
River chemistry
Nutrients
Seasonality
Weathering geochemistry

ABSTRACT

Thawing of permafrost and a shift in the timing of major seasonal transitions (spring melt and fall freeze-up) are two anticipated effects of climate warming in northern regions. These fundamental changes in terrestrial ecosystems could have major ramifications for the timing and fluxes of carbon and nutrient exports from watersheds and the geochemical signatures of northern rivers. Discontinuous permafrost, which underlies watersheds in Interior Alaska (USA), is expected to degrade rapidly in response to climate warming and this will likely alter subsurface flows and flow paths, water residence times, water-soil, and water-rock interactions. This study of the Chena River in Interior Alaska was undertaken to quantify dissolved organic carbon (DOC), total dissolved nitrogen (TDN), major ion, strontium isotope, and stable oxygen and hydrogen isotope values during two year-long time series sampling periods. Our goal was to identify the hydrogeochemical signatures associated with the major seasonal flow regimes. Periods of increased discharge such as spring melt and major summer precipitation events yielded elevated DOC and TDN concentrations, diluted major ion concentrations, and shifted stable oxygen and hydrogen isotope ratios from base flow toward precipitation values. During dry summer periods nutrient concentrations decreased and strontium isotope values were indicative of a higher proportion of silicate versus carbonate mineral dissolution. Winter base flow had a unique geochemical signal with a slight increase in TDN concentrations compared to typical summer conditions, and a lower proportion of silicate versus carbonate mineral dissolution. Since flow paths in subarctic watersheds can change dramatically over the course of a year we interpreted our results within the context of a schematic model for subsurface flow to identify how permafrost degradation might affect nutrient exports and hydrogeochemical patterns in these watersheds.

Published by Elsevier B.V.

1. Introduction

Interior Alaska is underlain by discontinuous permafrost which is predominantly found on north facing slopes, valley bottoms, and beneath poorly drained soils (Hamilton et al., 1983; Jorgenson et al., 2001). Permafrost acts as a confining bed in the subsurface that reduces soil water storage capacity and restricts flow paths (Hinzman et al., 1991, 1998; Kane et al., 1991; Woo, 2000). The presence of permafrost can greatly affect the stream discharge response to storm activity (Carey and Quinton, 2005), the geochemistry of stream flow (Petrone et al., 2006; Keller et al., 2010; Bagard et al., 2011), and the seasonal fluxes of nutrients including carbon and nitrogen out of northern watersheds (Carey, 2003; O'Donnell and Jones, 2006; Frey et al., 2007; Frey and McClelland, 2009).

Future climate scenarios predict a roughly 5 °C increase in mean annual air temperatures for the Alaskan Interior over the next 80 years (Chapman and Walsh, 2007). These increasing temperatures are expected to have pronounced effects in regions underlain by discontinuous permafrost (Osterkamp and Romanovsky, 1999). Large areas of permafrost in Interior Alaska have exhibited signs of degradation for the past 20 years (Racine and Walters, 1994; Jorgenson et al., 2001, 2006; Osterkamp, 2007) and this is expected to continue with additional climate warming (Marchenko et al., 2008). Permafrost degradation is typically associated with development of thermokarst (thaw induced degradation of permafrost) and formation of taliks (zones of unfrozen material created as permafrost thaws in areas below the seasonal freeze depth), and a thicker seasonally thawed (active) layer (Osterkamp and Jorgenson, 2006; Douglas et al., 2008). These changes in permafrost distribution and vertical extent could potentially alter ecosystems and the watersheds that drain them in largely unpredictable ways with widespread drying in some regions and wetland expansion in others (Racine and Walters, 1994; Osterkamp and Jorgenson, 2006).

* Corresponding author. Tel.: +1 907 361 9555; fax: +1 907 353 5142.
E-mail address: Thomas.A.Douglas@usace.army.mil (T.A. Douglas).
[1] Now at: Shell Exploration and Production, 190 Thorn Hill Road, Warrendale, PA 15086, USA.

0- 009-2541/$ – see front matter. Published by Elsevier B.V.
http://dx.doi.org/10.1016/j.chemgeo.2012.10.045

Between 400 and 450 Gt of carbon is currently estimated to be stored in syngenetically frozen permafrost in the northern hemisphere (Zimov et al., 2006a, 2006b; Tarnocai et al., 2009) and some of this carbon could be liberated as permafrost thaws (Petrone et al., 2006; Guo et al., 2007; Shur and Jorgenson, 2007). Arctic and sub-Arctic watersheds export much of their carbon as dissolved organic carbon (DOC) that is flushed out of surface vegetation and soils during spring melt (Guo and Macdonald, 2006; Cai et al., 2008a; Guo et al., 2012). Roughly 60% of the annual DOC export from major arctic rivers occurs within the two months following snowmelt and ice breakup (Finlay et al., 2006; Raymond et al., 2007). Carbon mobilized and transported out of watersheds at this time has been reported to be of modern age (Guo and Macdonald, 2006; Neff et al., 2006; Holmes et al., 2008). Spring melt also typically brings the largest surface water loads of nutrients (like nitrogen) and trace metals (Rember and Trefry, 2004; Stolpe et al., in press) as melt water interacts with surface soil and vegetation (McNamara et al., 2008; Frey and McClelland, 2009).

The intense seasonality of flow paths, discharge, and streamwater geochemistry is a unique characteristic of northern watersheds. Since permafrost currently acts as a confining layer the loss of permafrost from northern catchments will undoubtedly alter flow paths (Walvoord and Striegl, 2007; Bense et al., 2009) and the response of stream flows and biogeochemistry to seasonal events including spring melt runoff or summer storms (Thompson and Woo, 2009; Guo et al., 2012). Other anticipated changes in the subarctic terrestrial landscape include changes in the surface soil regime (Sierra et al., 2011), altered forest succession (Euskirchen et al., 2010; Wolken et al., 2011), and increased fire activity (Johnstone et al., 2010; Wendler et al., 2010). Collectively, these ecosystem changes could markedly alter the seasonality, geochemistry, and nutrient dynamics of watersheds underlain by permafrost and could shift the carbon balance of subarctic watersheds from a net sink to a net source (McGuire et al., 2009; Grosse et al., 2011). However, the specific ways in which these changes will affect the seasonality of carbon and nutrient export and river geochemistry in watersheds draining permafrost remain poorly understood, limiting our ability to develop predictive models for nutrient and geochemical processes and exports from northern watersheds.

This study was undertaken to measure the dissolved organic carbon (DOC), total dissolved nitrogen (TDN), major ions, strontium isotope, and stable oxygen and hydrogen isotope values of the Chena River of Interior Alaska during two separate year-long sampling periods. Samples were collected bi-weekly and represent a variety of major flow regimes including winter base flow, spring melt, summer dry periods and major summer rain events. The goals of the study were to quantify how geochemical signatures respond to flow regimes in the watershed and to identify what biogeochemical tracers were best suited for quantifying relationships between watershed hydrology and river geochemistry. Since future climate scenarios predict less permafrost in Interior Alaska we interpret our results within the context of a schematic model of the seasonality of flow paths to identify where the effects of climate warming on discontinuous permafrost may influence the sources and fluxes of carbon, nutrients, and geochemical tracers from northern watersheds.

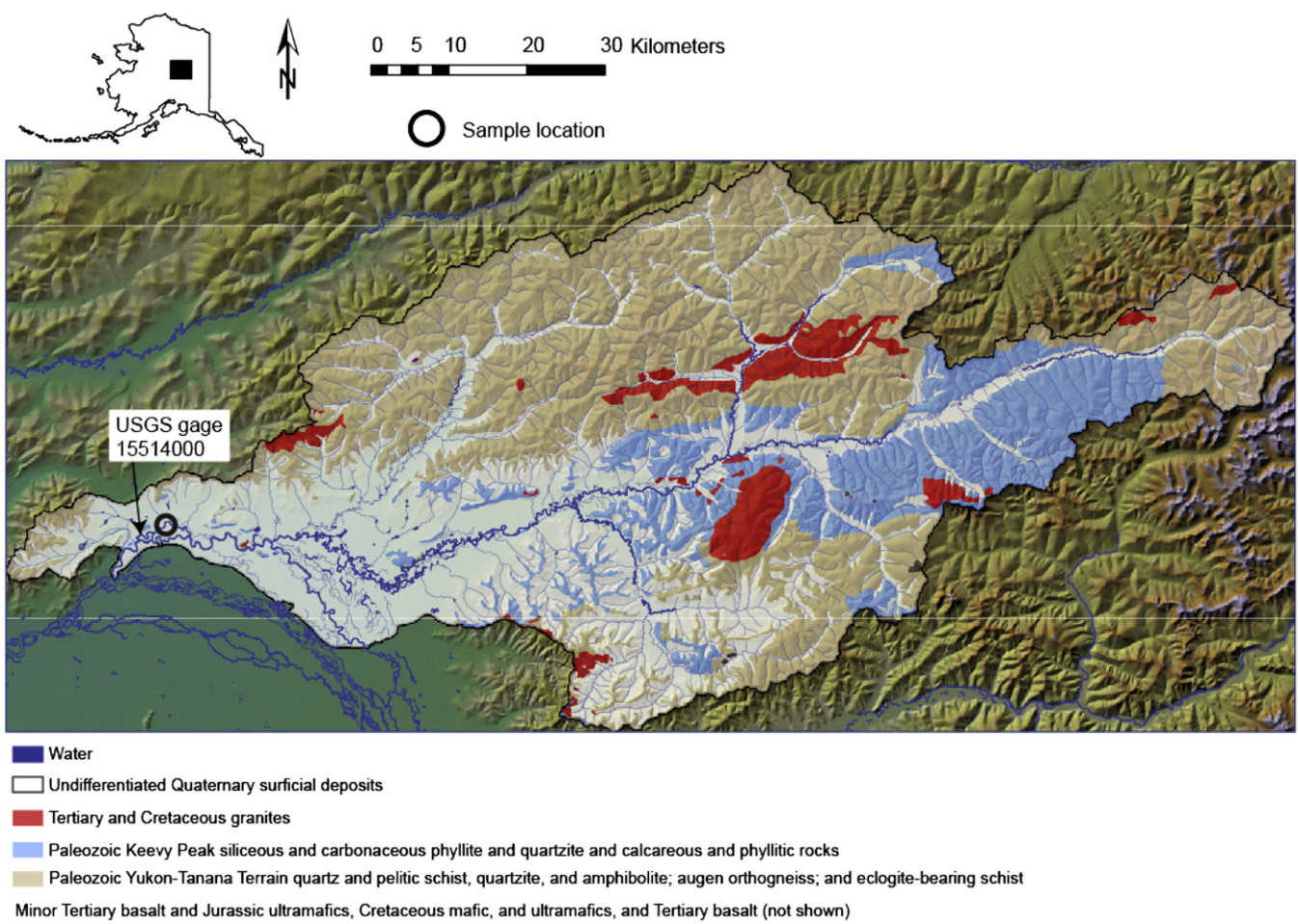

Fig. 1. A simplified geologic map of the Chena River watershed modified from Newberry et al. (1996), Wilson et al. (1998), and Douglas et al. (2002). The United States Geological Survey gaging station #15514000 (arrow) and our sampling location (circle) are identified.

2. Materials and methods

2.1. Climatic and geologic setting of the Chena River watershed

The Chena River (Fig. 1) drains an area of 5200 km^2 originating in the Yukon–Tanana uplands and flowing westward into the Tanana River at Fairbanks, Alaska (USA). Interior Alaska has a continental climate with a mean annual temperature of −3.3 °C and typical monthly average temperatures of 20.2 °C in the summer (July) and −31.7 °C in the winter (January) with extremes ranging from −51 °C to 38 °C (Jorgenson et al., 2001). With an average annual wet precipitation of 407 mm and a typical average annual snowfall of 1.7 m the total wet equivalent annual precipitation is 577 mm. The Chena River watershed is underlain by discontinuous permafrost which ranges from a few meters to over 50 m thick and is most commonly found on north facing slopes in the southern half of the watershed and in valley bottoms (Jorgenson et al., 2001). South facing and well-drained slopes, especially in upland regions and in the northern half of the watershed, tend to be free of permafrost (Osterkamp et al., 2000).

The entire watershed is located within the polygenetic Yukon–Tanana Terrane (YTT), which is bounded by the Tintina fault to the north and the Denali fault to the south (Hansen and Dusel-Bacon, 1998). Geology in the watershed includes predominantly low to medium grade metamorphic rocks that have been intruded by Cretaceous and Tertiary granitoid plutons (Blum, 1985). Minor Tertiary flood basalts are located in the watershed. Bedrock in the northern half of the watershed is predominantly composed of Paleozoic rocks of the YTT. This includes quartz and pelitic schist, quartzite, amphibolite, orthogneiss, and eclogite-bearing schist (Wilson et al., 1998; Douglas et al., 2002). The southern portion of the watershed has more north-facing slopes underlain by permafrost and contains Paleozoic siliceous and carbonaceous phyllite and quartzite rocks of the Keavy Peak Formation (Wilson et al., 1998). These rocks contain more carbonate-bearing lithologies than the Paleozoic metamorphic rocks in the northern portion of the watershed. However, the YTT rocks also contain disseminated calcite and minor bands of marble (Newberry et al., 1996). The watershed remained unglaciated during the Quaternary and low-lying elevations and valley bottoms are typically covered by unconsolidated Quaternary fluvial deposits and Quaternary loess (Karlstrom et al., 1964; Kauman and Manley, 2004).

2.2. Chena River flow regimes

Discharge in the Chena River (Fig. 2, top panel) typically consists of a large spring melt event in late April that lasts for a few weeks and generally provides the largest annual flows. The summer season is characterized by intermittent dry and wet periods. Fall freeze-up occurs in late October and base flow dominates from November to April. Most of the river remains ice covered throughout the winter with ice up to one meter thick.

We collected water samples from the Chena River upstream of Fairbanks, Alaska from March 2005 to March 2006 and from March 2008 to March 2009. Samples were generally collected bi-weekly but we also collected additional samples representing spring melt runoff, extreme summer dry periods, and major precipitation events. Samples were collected from a location (64.835°N; 147.648°W) 3 km upstream of the United States Geological Survey gage #15514000 on the Chena River. No tributaries flow into the river between our sampling location and the gage. Our sampling location was located 2 km upstream of the urban center of Fairbanks to avoid potential influence from human activities and 10 km upstream of the confluence of the Chena and Tanana Rivers. The U.S. Army Corps of Engineers operates a flood control diversion dam 20 km upstream of our sampling site, but it is only used during extreme flow events and was not used during either of the two years for which we collected samples. As a result our samples represent a relatively pristine, undammed, and undiverted river system.

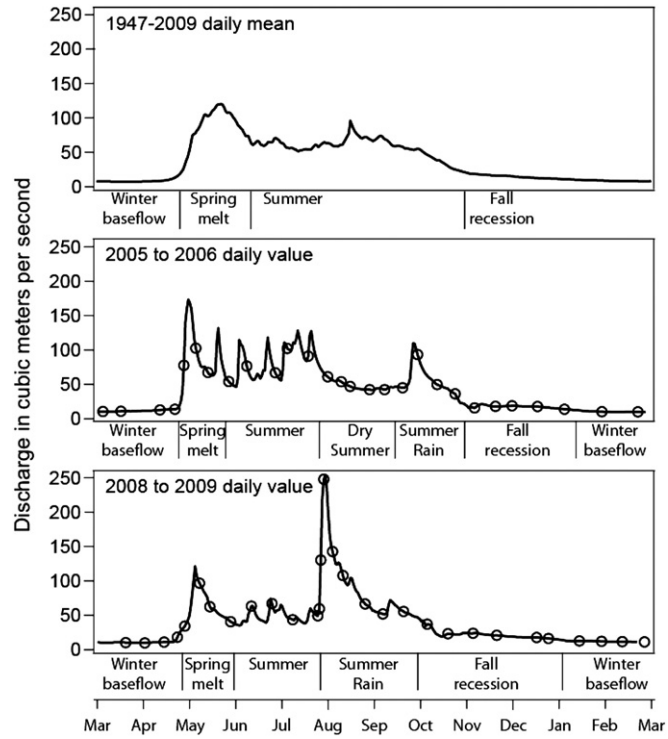

Fig. 2. Upper panel: mean daily discharge in the Chena River from the United States Geological Survey gage #1551400 above downtown Fairbanks. Middle panel: mean daily discharge from March 2005 to March 2006; sample events are denoted by the circles. Lower panel: mean daily discharge from March 2008 to March 2009; sample events are denoted by the circles.

2.3. Sample collection procedures

Samples were collected along a 1 km long straight section of river near a bridge spanning the river channel. In the summer a 3 L high density polyethylene (HDPE) bucket on a rope was used to collect water from three locations across the bridge. These samples represented the bulk of flow in the river. The water was mixed into a 10 L HDPE carboy and samples for our different measurement techniques were subsampled at our laboratory 1 km away. When the river was ice covered we used a 10 cm diameter gas powered corer to drill holes through the ice slightly downstream of the bridge at three locations across the river. One liter HDPE bottles were dipped into the holes in the ice and used to collect 5 L of flowing water from each location. The water was mixed into a 20 L HDPE carboy which was brought to the laboratory for processing and subsampling. In the summer we measured water temperature, specific conductivity, and turbidity at an accessible location along the main river channel on the north side of the bridge using portable meters. In the winter these parameters were measured from the flow beneath the three ice holes and the mean values were reported.

Samples for the nutrients TDN and DOC were filtered through 0.45 μm Millipore HTTP filters. Filtrates were collected and stored frozen for nutrient analysis. A separate set of samples, for strontium isotope and cation measurements, was filtered to less than 0.45 μm into 250 mL acid-washed HDPE bottles and were acidified to pH 2 using nitric acid. Samples for anion analysis were filtered through 0.45 μm HDPE syringe filters into 60 mL HDPE bottles. Samples for stable oxygen and hydrogen isotopes were filtered to less than 0.45 μm and stored in 60 mL HDPE bottles.

2.4. Dissolved organic carbon and total dissolved nitrogen measurements

Concentrations of DOC and TDN were measured in the Department of Marine Science at the University of Southern Mississippi using a high-temperature combustion total organic carbon analyzer (Shimadzu TOC-V) interfaced with a nitrogen detector (TNM-1; Guo and Macdonald, 2006; Cai et al., 2008a,b). The total DOC blank (including Milli-Q water, acid for sample acidification, and the instrument blank) was generally less than 6 μM. During sample analysis Nanopure water, working DOC standards and certified DOC standards (purchased from the University of Miami) were measured as samples every 8–10 samples to monitor instrument performance (Zhou and Guo, 2012). Precision was better than 2% and accuracy was within 1% based on the analysis of working standards.

2.5. Major anion and alkalinity measurements

Concentrations of the anions F, Cl, NO_3, and SO_4 were quantified on a Dionex ICS-3000 ion chromatograph with an AS-19 anion column (Dionex Corporation Sunnyvale, California) using a 10 mL injection volume. The analysis was carried out in the Geochemistry Laboratory at the Cold Regions Research and Engineering Laboratory, Alaska. A gradient method using potassium hydroxide eluent ranging from 20 to 35 mM was used for anion analyses. The system flow rate was 1 mL/min and the operating temperature was 30 °C. The ion chromatograph was calibrated through repeat analysis of five working standards with concentrations ranging from 0.5 to 120 mg/L (within the range of analyses). Laboratory analytical anion standards with values from 0.25 to 100 mg/L were analyzed repeatedly to verify system calibration and assess analytical precision. Based on these analyses the calculated precision for the analyses was ±5%. Peaks were identified using Chromeleon software (Dionex, Sunnyvale, California) and were verified visually.

Carbonate alkalinity was measured by Gran titration (Stumm and Morgan, 1996) from 40 mL of water at 25 °C. The initial pH was noted for each sample, 1 mL aliquots of 20 mM hydrochloric acid were added to the sample and the pH was measured following each acid addition. After roughly 10 acid additions the pH decreased to below 3 and the Gran function was calculated for each pH measurement. The x-intercept of a plot of the volume of acid added versus the Gran function was used to calculate alkalinity. Repeat analyses of duplicate samples yielded an analytical precision for the alkalinity measurements of 10%.

2.6. Cation and strontium isotope measurements

Concentrations of the cations Na, K, Mg, Ca, Sr, Ba, and Si were measured in the Department of Earth and Environmental Sciences at the University of Michigan by inductively coupled plasma optical emission spectrometry (ICP-OES) using five-point calibration curves. One in-house standard and two National Institute of Standards and Technology traceable commercial standards were used for quality control. These standards were analyzed to within ±7% of the known values for all seven cations. For isotope analysis Sr was separated by elution through a Sr-specific resin (Eichrom) in quartz cation exchange columns and approximately 75 ng of Sr was loaded onto a tungsten filament with Ta_2O_5 powder. The Sr isotope ratio was determined by thermal ionization mass spectrometry using a Finnigan MAT 262. The internal precision (±2σ) of 100–200 ratios for each sample was less than ±0.000035, and replicate analyses of NBS987 yielded $^{87}Sr/^{86}Sr$ of 0.710231 ± 0.000016 (2σ, n = 112) during the period of analyses.

2.7. Hydrogen and oxygen stable isotope measurements

Stable isotopes of hydrogen and oxygen were measured using a Thermo Delta V mass spectrometer interfaced with a high temperature conversion elemental analyzer pyrolysis oven (Thermo Scientific Waltham, Massachusetts) at the University of Alaska Fairbanks Stable Isotope Facility. We report mean values of the triplicate analyses. Multiple analyses of standards and replicate analyses of samples yielded a precision generally better than ±0.4‰ for oxygen ($\delta^{18}O$) and ±2.0‰ for hydrogen isotopes (δD). Data are reported in per mil (‰) referenced to VSMOW.

3. Results

3.1. River flow regimes

Yearly peak flows in the Chena River typically occur in May and are driven by snow melt runoff (Fig. 2, upper panel). Summer discharge (mid-June to the end of October) is controlled by alternating low flows during dry periods and high flows following precipitation events. Winter base flow is initiated in late October and November and from then to early May there is little to no snow melt in Interior Alaska, as air temperatures remain consistently below 0 °C. The Chena River remains ice covered throughout the winter except for a few restricted locations where channels open intermittently. During the March 2005 to March 2006 sampling period (Fig. 2, middle panel) a typical spring melt event in early May was followed by alternating wet and dry periods common during Interior Alaska summers. However, from late July through September 2005 the region experienced extremely dry conditions. August, 2005 had the lowest monthly total precipitation since 1948 when record keeping was initiated (Alaska Climate Research Center, 2011) and during the summer of 2005 the area experienced the third largest area burned by forest fires since record-keeping was initiated in 1956 (Wendler et al., 2010). Flows during this extremely dry period likely represent summer base flow with some storage coming from seasonal thaw of the permafrost active layer and/or melting permafrost at depth. This dry period ended with a major rainfall event in early October and then the river experienced base flow recession toward the winter. The eight week period of extremely dry conditions was clearly an unusual event.

The 2008 to 2009 sampling year (Fig. 2, lower panel) exhibited spring melt peak runoff in early May followed by a few months of interspersed rain events and dry periods. In the middle of August Interior Alaska experienced an anomalously large rain event with more than 107 mm of precipitation falling over the watershed over a two week period. This is more than one quarter of the yearly mean rainfall for the area and led to three weeks of anomalously high discharge rates for the Chena River. Flows peaked at more than twice the typical spring melt maximum discharge. This was an unusual precipitation event. Following this extremely wet period the fall recession period started in early October.

Based on meteorology and discharge information for the Chena River during both sampling periods we identified six unique flow regimes for water samples. These include the four flow regimes that occur every year in northern watersheds: winter base flow, spring melt runoff, typical summer conditions, and fall recession. We identified two additional flow regimes during our sampling program: the extremely dry summer period in 2005 and the major summer rainstorm in 2008. We collected at least three individual samples during each of these flow regimes.

3.2. Dissolved organic carbon and total dissolved nitrogen

Tables 1 through 4 include discharge, temperature, turbidity, DOC, TDN, pH, major ion, alkalinity, trace element, $^{87}Sr/^{86}Sr$, and stable oxygen and hydrogen isotope values for all of our Chena River samples. Some of this information is displayed in Figs. 3 and 4. Concentrations of DOC in Chena River waters varied from 207 μM in winter to 1187 μM during spring melt runoff in the 2005–2006 sampling year and from 201 μM in winter to 1212 μM during peak spring melt

Table 1
Temperature, turbidity, pH, $^{87}Sr/^{86}Sr$, $\delta^{18}O$, δD, and dissolved organic carbon and total dissolved nitrogen concentrations measured in Chena River waters collected in 2005 and 2006.

Date collected	Flow regime	Discharge (m^3/s)[a]	T (°C)	Turbidity (NTU)	pH	$^{87}Sr/^{86}Sr$	$\delta^{18}O$ (‰)	δD (‰)	DOC (μM)[b]	TDN (μM)[b]	DOC/TDN
3/4/2005	Winter	7.65	0.2	1498.9	7.1	0.721406	−22.3	−155.6	207	26.4	7.9
3/16/2005	Winter	7.93	0.2	1481.2	7.2	0.721586	−21.9	−154.9	208	25.6	8.1
4/11/2005	Winter	9.91	0.3	1440.4	6.7	0.722027	−21.8	−155.6	210	23.9	8.8
4/21/2005	Winter	11.04	0.3	1474.0	6.9	0.722023	−21.3	−154.1	300	26.0	11.5
4/27/2005	Spring melt	76.46	0.4	755.7	4.8	0.725524	−22.9	−163.0	1187	50.7	23.4
5/5/2005	Spring melt	102.22	5.1	900.7	5.4	0.724871	−22.4	−163.4	896	36.3	24.7
5/13/2005	Spring melt	65.98	9.3	1071.7	6.6	0.724671	−22.4	−157.5	468	29.1	16.1
5/27/2005	Summer	52.39	11.1	1215.6	7.4	0.724005	−21.8	−156.6	417	26.1	16.0
6/8/2005	Summer	75.32	12.3	1094.8	6.8	0.725061	−21.4	−153.2	467	28.4	16.4
6/27/2005	Summer	65.41	12.2	1184.3	7.0	0.724491	−21.1	−152.1	392	27.9	14.0
7/5/2005	Summer	101.66	11.7	988.0	6.6	0.726227	−20.8	−150.5	576	32.2	17.9
7/19/2005	Summer	90.33	11.5	1134.5	7.0	0.725658	−21.0	−152.6	373	28.1	13.3
8/1/2005	Summer dry	59.47	10.0	1241.3	6.9	0.725387	−20.3	−149.9	318	30.9	10.3
8/10/2005	Summer dry	52.10	12.6	1251.0	7.8	0.725287	−20.9	−152.6	306	19.8	15.5
8/16/2005	Summer dry	45.02	12.3	1291.1	8.1	0.724836	−20.8	−152.0	298	16.7	17.8
8/29/2005	Summer dry	40.21	9.9	1304.1	7.2	0.724751	−21.2	−151.3	298	16.3	18.3
9/8/2005	Summer dry	40.21	8.8	1331.5	7.8	0.724570	−20.8	−152.6	310	18.5	16.7
9/20/2005	Summer rain	43.04	7.1	1337.6	7.9	0.724387	−20.7	−150.6	352	22.6	15.5
9/30/2005	Summer rain	92.60	3.5	1177.1	6.7	0.725261	−20.5	−148.3	648	40.1	16.2
10/13/2005	Summer rain	47.86	0.3	1311.4	7.4	0.724506	−19.4	−147.9	323	31.6	10.2
10/25/2005	Summer rain	33.98	0.1	1355.9	7.7	0.723350	−20.7	−152.8	265	30.3	8.8
11/7/2005	Fall recession	13.03	0.1	1565.6	7.9	0.723345	−21.0	−155.1	281	30.1	9.3
11/21/2005	Fall recession	15.29	0.1	1398.1	7.4	0.723050	−21.0	−154.1	235	27.2	8.6
12/2/2005	Fall recession	16.14	0.1	1418.0	7.7	0.723773	−22.3	−155.2	222	28.6	7.8
12/19/2005	Fall recession	15.01	0.1	1402.4	7.3	0.723390	−22.3	−153.7	214	28.3	7.6
1/6/2006	Winter	11.04	0.1	1465.2	7.2	0.723251	−23.1	−155.1	223	30.6	7.3
1/31/2006	Winter	7.36	0.1	1507.2	7.2	0.722178	−21.3	−156.4	234	–	–
2/24/2006	Winter	7.08	0.1	1499.4	6.8	0.721205	−21.8	−156.4	236	–	–

[a] Cubic meters per second.
[b] From Cai et al. (2008a).

runoff in the 2008–2009 sampling year. Values were typically lowest during winter base flow conditions or dry summer periods and were highest during spring melt or immediately following summer precipitation events. Total dissolved nitrogen concentrations show a similar distribution trend as DOC with peak values during spring melt runoff or summer rain events (Fig. 5). However, while DOC was lowest during winter low stream flow periods the TDN concentrations remained high during the winter.

Table 2
Major ion concentrations measured in Chena River waters collected in 2005 and 2006.

Date collected	Sodium (μM/L)	Potassium (μM/L)	Magnesium (μM/L)	Calcium (μM/L)	Strontium (μM/L)	Barium (μM/L)	Silica (μM/L)	Fluoride (μM/L)	Chloride (μM/L)	Nitrate (μM/L)	Sulfate (μM/L)	HCO_3^- (μM/L)	Σ+ (μeq/L)[a]	Σ− (μeq/L)[b]
3/4/2005	165.7	47.0	288.4	749.5	1.65	0.44	268.8	7.06	50.5	11.4	198.1	1967	2288	2471
3/16/2005	162.4	45.4	285.8	740.6	1.63	0.42	257.4	7.21	47.2	14.6	201.4	1980	2261	2501
4/11/2005	156.4	44.6	277.0	720.2	1.59	0.38	238.5	6.66	45.3	11.9	207.6	1954	2195	2474
4/21/2005	155.3	44.5	280.2	737.0	1.64	0.38	236.9	6.94	42.2	11.9	220.2	1700	2234	2243
4/27/2005	70.8	61.5	157.3	377.9	0.93	0.23	107.2	4.82	24.3	16.7	191.7	901	1203	1388
5/5/2005	72.3	31.7	177.6	450.3	1.09	0.19	117.1	5.39	16.7	17.1	201.9	888	1360	1390
5/13/2005	89.4	31.1	202.4	535.9	1.28	0.22	144.7	6.61	18.8	18.0	226.0	1066	1597	1623
5/27/2005	108.1	33.8	226.8	607.8	1.45	0.27	171.0	7.42	24.7	17.1	233.5	1273	1811	1848
6/8/2005	90.1	27.9	199.5	547.4	1.29	0.21	147.5	6.83	16.7	19.8	216.7	1066	1612	1611
6/27/2005	99.7	29.3	217.2	592.1	1.42	0.24	162.8	7.02	19.0	20.9	212.4	1167	1748	1711
7/5/2005	82.3	24.4	184.6	494.0	1.24	0.18	158.3	6.59	13.2	22.9	183.6	1155	1464	1643
7/19/2005	91.9	28.1	200.2	567.2	1.35	0.21	155.6	6.96	17.0	20.0	207.4	1128	1655	1655
8/1/2005	102.8	31.4	215.8	620.7	1.46	0.23	157.5	6.86	18.9	16.4	204.6	1114	1807	1621
8/10/2005	106.7	32.9	222.5	625.5	1.51	0.24	129.4	7.80	19.5	11.7	228.0	1382	1835	1917
8/16/2005	113.9	34.7	231.1	645.5	1.55	0.26	124.7	8.07	23.6	9.7	229.6	1220	1902	1753
8/29/2005	115.0	35.0	237.9	652.1	1.57	0.26	128.4	7.18	22.5	8.2	219.4	1396	1930	1901
9/8/2005	114.0	34.8	240.2	665.8	1.59	0.26	142.7	7.77	22.4	10.7	245.0	1551	1961	2119
9/20/2005	110.8	33.9	244.3	668.8	1.61	0.25	148.3	7.90	20.6	13.2	253.0	1417	1971	2010
9/30/2005	81.2	25.6	213.2	588.5	1.39	0.19	152.0	6.74	12.8	24.0	241.4	1227	1710	1835
10/13/2005	108.1	32.1	238.5	655.7	1.55	0.25	178.6	7.42	21.2	21.7	250.6	1389	1929	2015
10/25/2005	114.8	33.7	248.0	678.0	1.59	0.27	186.1	7.74	24.6	21.8	251.1	1551	2000	2182
11/7/2005	156.1	45.1	285.9	782.8	1.78	0.40	248.0	7.89	36.5	17.6	239.9	1904	2339	2506
11/21/2005	135.8	39.4	259.5	699.0	1.60	0.37	217.7	7.41	34.1	17.3	234.1	1748	2092	2335
12/2/2005	131.0	37.6	260.4	709.0	1.62	0.34	213.3	7.72	29.7	19.6	245.9	1622	2108	2237
12/19/2005	130.9	37.0	257.0	701.2	1.58	0.32	211.1	7.35	31.0	18.7	238.2	1664	2084	2261
1/6/2006	135.3	36.5	285.6	732.6	1.65	7.60	236.0	7.21	37.3	17.3	221.1	1650	2208	2213
1/31/2006	154.9	42.5	302.5	753.6	1.67	14.88	278.9	7.19	53.9	10.6	193.9	2045	2310	2540
2/24/2006	167.8	43.1	302.8	749.7	1.71	22.16	278.2	6.77	54.3	12.9	177.5	1904	2316	2377

[a] The sum of sodium, potassium, magnesium, and calcium in microequivalents per liter.
[b] The sum of fluoride, chloride, nitrate, sulfate, and bicarbonate in microequivalents per liter.

Table 3
Temperature, turbidity, pH, $^{87}Sr/^{86}Sr$, $\delta^{18}O$, δD, and dissolved organic carbon and total dissolved nitrogen concentrations measured in Chena River waters collected in 2008 and 2009.

Date	Flow regime	Discharge (m^3/s)[a]	T (°C)	Turbidity (NTU)	pH	$^{87}Sr/^{86}Sr$	$\delta^{18}O$ (VSMOW) (‰)	δD (VSMOW) (‰)	DOC (μM)	TDN (μM)	DOC/TDN
3/20/2008	Winter	6.51	0.1	8.2	7.0	0.720474	−21.6	−158.5	206	33.5	6.1
4/2/2008	Winter	5.95	0.1	8.9	6.7	0.720436	−21.6	−158.1	208	31.6	6.6
4/15/2008	Winter	7.36	0.1	7.2	6.6	0.720293	−19.9	−158.5	206	31.2	6.6
4/24/2008	Winter	14.72	0.3	11.0	6.8	0.720686	−19.5	−157.9	284	30.6	9.3
4/29/2008	Spring melt	31.15	0.3	13.0	7.4	0.725155	−21.9	−161.0	745	32.0	23.3
5/9/2008	Spring melt	76.74	3.9	26.0	7.4	0.724632	−22.2	−164.5	1188	37.1	32.0
5/16/2008	Spring melt	56.92	6.8	11.5	7.5	0.724124	−22.0	−159.5	561	28.1	19.9
5/30/2008	Spring melt	35.40	9.5	4.2	7.4	0.723542	−21.6	−156.0	321	23.9	13.4
6/13/2008	Summer	59.47	10.7	7.8	7.3	0.725154	−21.6	−155.0	612	31.9	19.2
6/27/2008	Summer	62.86	12.2	22.5	7.4	0.723223	−21.1	−152.6	796	33.1	24.1
7/11/2008	Summer	39.08	14.4	4.0	7.5	0.723666	−21.4	−152.7	409	25.7	15.9
7/28/2008	Summer	44.17	11.5	2.6	7.4	0.723653	−21.3	−152.8	318	23.3	13.7
7/29/2008	Summer rain	56.35	11.9	4.2	7.5	0.723827	−21.9	−153.3	332	23.7	14.0
7/30/2008	Summer rain	124.03	8.7	61.0	7.2	0.723697	−21.7	−150.4	818	35.1	23.3
8/1/2008	Summer rain	255.13	7.1	41.0	7.2	0.723996	−21.6	−148.5	1212	41.1	29.5
8/7/2008	Summer rain	139.89	7.9	12.2	7.3	0.724689	−21.7	−149.9	641	46.3	13.8
8/14/2008	Summer rain	102.79	9.9	6.8	7.3	0.724850	−21.4	−151.3	480	38.6	12.4
8/29/2008	Summer rain	62.01	8.3	5.1	7.5	0.724214	−21.8	−151.6	319	30.9	10.3
9/10/2008	Summer rain	47.86	7.6	3.1	7.4	0.723992	−22.3	−151.8	276	24.8	11.1
9/24/2008	Summer rain	52.10	3.4	2.5	7.3	0.723718	−21.9	−151.8	308	28.0	11.0
10/10/2008	Fall recession	36.53	0.5	2.5	7.2	0.722914	−22.0	−152.8	262	29.2	9.0
10/24/2008	Fall recession	19.82	0.1	2.5	7.4	0.723057	−21.9	−153.0	239	31.4	7.6
11/10/2008	Fall recession	20.39	0.1	4.2	7.2	0.723020	−21.8	−153.1	216	33.0	6.5
11/26/2008	Fall recession	17.56	0.1	4.9	7.0	0.722951	−21.4	−153.0	204	32.9	6.2
12/23/2008	Fall recession	14.16	0.1	5.9	6.8	0.722815	−22.2	−153.1	206	39.6	5.2
12/31/2008	Fall recession	12.74	0.1	6.1	6.9	0.722772	−22.4	−153.2	201	32.7	6.1
1/21/2009	Winter	9.06	0.1	7.1	7.0	0.721428	−22.2	−154.1	204	31.9	6.4
2/5/2009	Winter	8.50	0.1	7.7	7.0	0.721221	−23.3	−154.1	205	30.6	6.7
2/19/2009	Winter	7.93	0.1	7.7	6.9	0.720883	−23.2	−154.2	210	33.1	6.3
3/6/2009	Winter	7.65	0.1	8.0	7.0	0.720659	−23.1	−155.1	218	34.1	6.4

[a] Cubic meters per second.

Table 4
Major ion concentrations measured in Chena River waters collected in 2008 and 2009.

Date collected	Sodium (μM/L)	Potassium (μM/L)	Magnesium (μM/L)	Calcium (μM/L)	Strontium (μM/L)	Barium (μM/L)	Silica (μM/L)	Fluoride (μM/L)	Chloride (μM/L)	Nitrate (μM/L)	Sulfate (μM/L)	HCO_3^- (μM/L)	Σ+ (μeq/L)[a]	Σ− (μeq/L)[b]
3/20/2008	158.3	42.3	259.0	665.4	1.36	0.37	70.4	6.2	74.1	7.2	152	2449	2049	2865
4/2/2008	202.4	53.8	336.3	865.7	1.78	0.51	144.2	7.51	70.9	7.2	145.8	2624	2087	3025
4/15/2008	199.0	53.2	334.6	850.6	1.74	0.48	136.9	6.72	69.2	6.1	164.8	2441	2622	2873
4/24/2008	164.5	58.2	267.6	664.7	1.37	0.35	81.8	6.98	67.6	7.2	169.7	1844	2659	2290
4/29/2008	115.5	46.1	224.3	562.6	1.29	0.20	32.8	5.93	24.6	11.3	225.7	1240	1735	1772
5/9/2008	88.7	37.1	161.8	438.0	0.99	0.16	20.1	5.25	15.3	10.1	163.5	843	2044	1235
5/16/2008	107.5	35.2	213.7	557.6	1.25	0.19	27.9	6.61	19.6	12.3	212.1	1582	1685	2087
5/30/2008	131.4	37.2	257.0	681.0	1.51	0.25	81.5	6.45	28.5	9.7	232.6	1550	1325	2093
6/13/2008	107.6	31.2	196.7	545.3	1.27	0.16	25.9	6.66	16.3	14.1	202.9	1161	1622	1652
6/27/2008	99.5	29.1	199.6	532.1	1.21	0.16	34.8	7.7	12.1	12.8	187.3	1129	1592	1580
7/11/2008	128.4	35.3	243.0	646.4	1.46	0.23	49.2	6.03	23.7	8.6	199.4	1281	1942	1748
7/28/2008	123.6	35.6	244.4	685.2	1.52	0.22	44.9	7.7	22.1	10.6	241.1	1383	2018	1942
7/29/2008	115.3	34.0	227.7	650.0	1.43	0.19	53.4	6.45	20.1	13.6	245.3	1518	1904	2095
7/30/2008	97.6	28.9	189.2	504.2	1.17	0.17	27.8	7.18	7.0	14.1	195	1106	1075	1572
8/1/2008	81.6	28.5	131.1	351.5	0.78	0.15	35.1	6.22	7.6	14.1	139	628	1426	982
8/7/2008	95.1	28.0	173.4	478.0	1.07	0.15	58.2	6.24	12.8	21.4	185.5	1256	1925	1741
8/14/2008	111.6	31.6	201.8	555.9	1.29	0.18	47.4	5.79	15.7	21.3	201.3	1232	2064	1751
8/29/2008	123.1	35.4	230.9	652.5	1.46	0.22	67.2	6.74	22.4	18.2	213.6	1288	2211	1825
9/10/2008	136.7	37.7	253.1	695.1	1.59	0.25	62.9	6.91	26.4	13.6	225.6	1208	2237	1753
9/24/2008	126.2	36.1	248.6	702.4	1.54	0.22	48.5	6.57	24.3	15.9	243.5	1320	2239	1908
10/10/2008	139.0	38.9	268.7	747.9	1.61	0.27	70.3	7.02	32.6	15.6	241.2	1375	1513	1967
10/24/2008	147.1	40.6	275.6	749.4	1.61	0.31	80.3	6.16	35.4	14.7	221.6	1574	1658	2124
11/10/2008	146.8	40.1	277.3	749.1	1.61	0.32	137.3	6.49	41.5	20.8	234.4	1447	2070	2056
11/26/2008	152.6	40.1	282.1	741.1	1.65	0.32	109.7	6.28	36	17.1	220.7	1577	2239	2136
12/23/2008	162.9	42.7	288.2	758.8	1.68	0.33	108.1	5.34	43.7	17.4	220	1312	2299	1878
12/31/2008	163.8	42.3	294.7	762.9	1.70	0.35	130.5	6.37	43	17.1	219.3	1458	2321	2021
1/21/2009	174.5	46.3	302.7	771.7	1.68	0.41	197.9	5.88	55.4	11.4	193.9	1564	2369	2063
2/5/2009	176.8	45.7	316.8	794.4	1.72	0.42	128.8	8.34	56.5	12	194.3	1577	2444	2083
2/19/2009	183.3	47.5	321.3	817.3	1.75	0.44	178.3	7.96	62.6	11	191	1472	2507	1973
3/6/2009	189.6	49.3	327.7	826.1	1.76	0.46	207.1	6.85	67	10.8	184.1	1577	2546	2067

[a] The sum of sodium, potassium, magnesium, and calcium in microequivalents per liter.
[b] The sum of fluoride, chloride, nitrate, sulfate, and bicarbonate in microequivalents per liter.

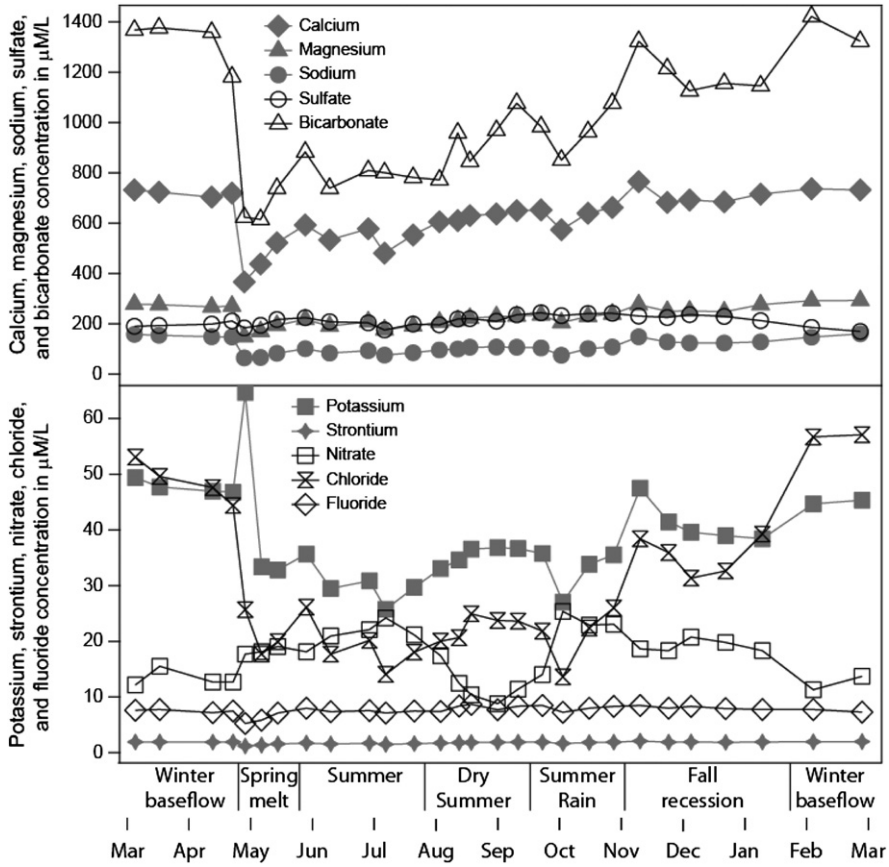

Fig. 3. Variations in major ion concentrations in the Chena River during the 2005–2006 sampling period.

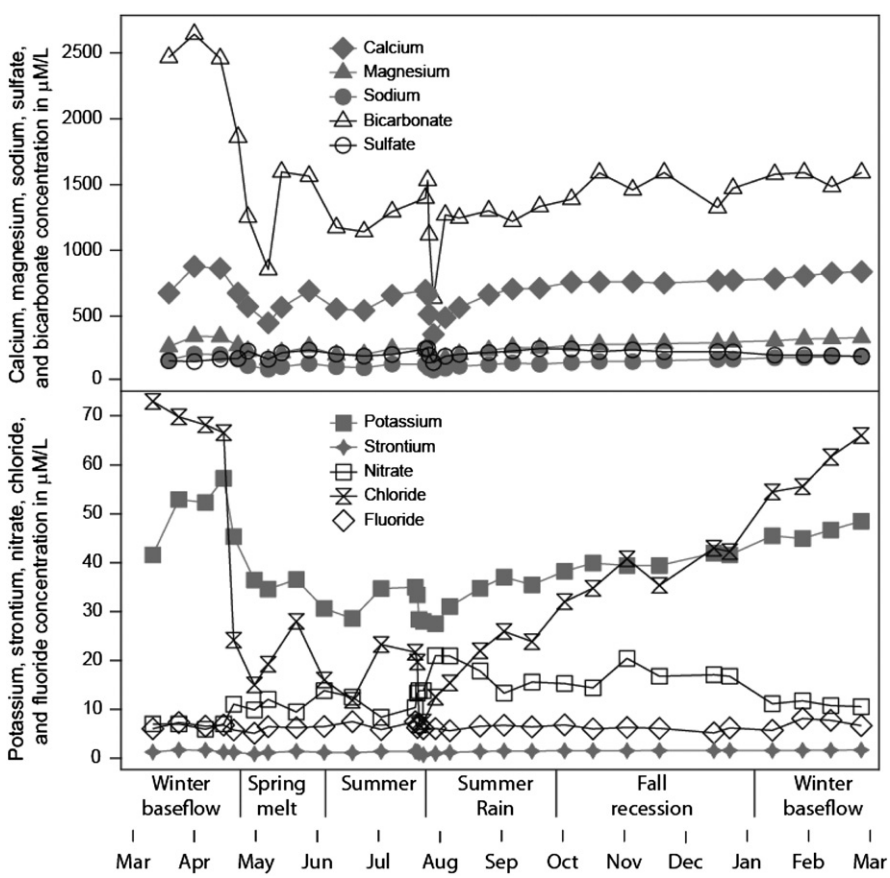

Fig. 4. Variations in major ion concentrations in the Chena River during the 2008–2009 sampling period.

Mean DOC and TDN concentrations during the 2008–2009 sampling period (414 ± 286 μM for DOC and 32 ± 5 μM for TDN) were not statistically different from values measured during the 2005–2006 sampling period (374 ± 222 μM for DOC and 28 ± 7 μM for TDN). In addition, the mean DOC to TDN ratios were similar during the two distinct year-long sampling periods (13 ± 5 during 2005–2006 and 13 ± 8 during 2008–2009) although their seasonal variations were slightly different.

3.3. Major ions and alkalinity

Figs. 3 and 4 show the variations in the major ion concentrations during the two sampling years. Ca, Mg, Na, K, HCO_3, and Cl yield their highest concentrations in the late winter base flow immediately prior to spring melt. For the most part these elevated concentrations are also evident in early winter flows at the end of the fall recession period. All of the major ions except NO_3 and K yield their lowest yearly values during peak spring melt and low concentrations are also evident during and following major summer precipitation events. The major ion concentrations (except for NO_3) increased steadily during the extremely dry period in 2005 and the values decreased markedly immediately following the major rain event. In the summer of 2008 the link between decreased major ion concentrations (except NO_3) and rain events is evident.

Nitrate behaved oppositely to the other major ions during both year-long sampling periods. There was a sharp increase in river water NO_3 concentrations during spring melt and immediately following most rain events. Nitrate values decreased during dry periods and increased following rain events. The lowest non-wintertime NO_3 concentrations were measured for the dry period in the summer of 2005 while the highest NO_3 concentrations were measured from flows during the early October 2005 rain event that ended this period of extremely dry conditions. In the summer of 2008 the highest NO_3 concentrations were measured following the major rain event in early August.

3.4. Strontium isotopes and Ca/Sr ratios

Fig. 6 includes a plot of $^{87}Sr/^{86}Sr$ ratios versus discharge. The yearly range in $^{87}Sr/^{86}Sr$ values is similar during both yearlong sample periods.

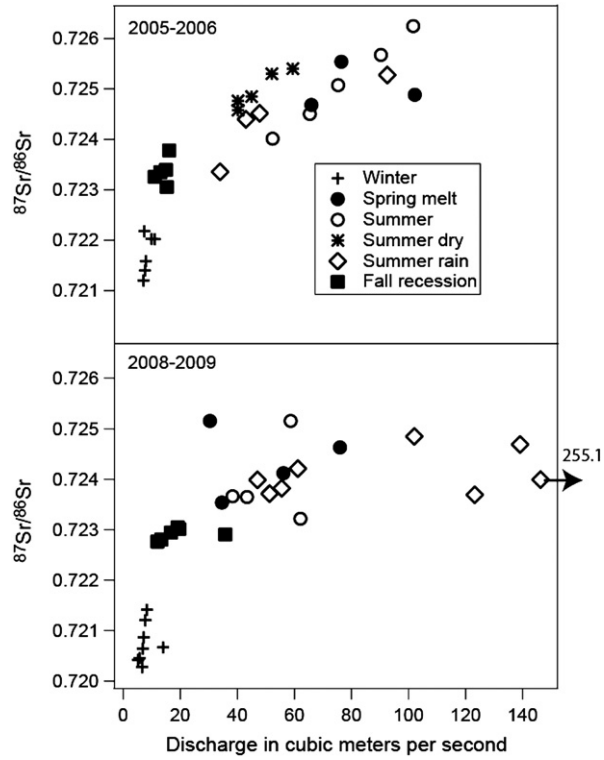

Fig. 6. $^{87}Sr/^{86}Sr$ versus discharge for the Chena River in 2005–2006 (upper panel) and 2008–2009 (lower panel).

$^{87}Sr/^{86}Sr$ ratios are lowest during winter base flow for both sampling years. Fall recession $^{87}Sr/^{86}Sr$ ratios are generally intermediate between the winter season values and the values from water collected during all other seasons. For spring melt, summer, summer dry, and fall recession samples the $^{87}Sr/^{86}Sr$ ratios increased with increasing discharge. However, the 2008 major rain event was associated with $^{87}Sr/^{86}Sr$ ratios that were not correlated with discharge.

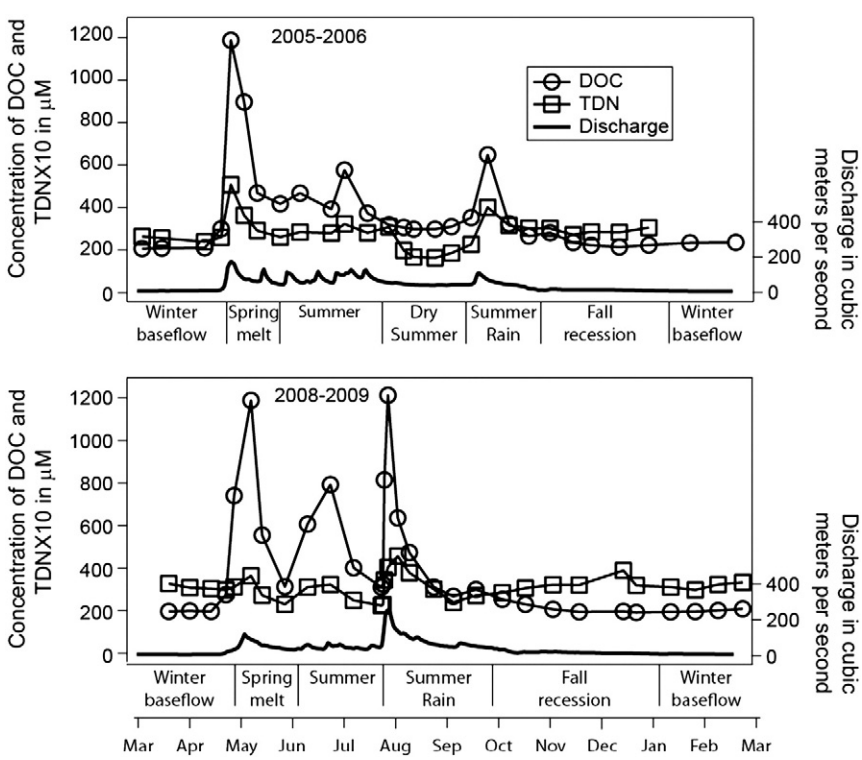

Fig. 5. Concentrations of dissolved organic carbon (DOC) and total dissolved nitrogen (TDN) × 10 versus discharge for 2005–2006 (upper panel) and 2008–2009 (lower panel).

The link between $^{87}Sr/^{86}Sr$ ratios and cation ratios (as represented by Ca/Sr values) in Chena River water is depicted in Fig. 7. There is a trend of higher $^{87}Sr/^{86}Sr$ ratios with decreasing Ca/Sr values for both years. The relationship is stronger in the 2005–2006 period than in the 2008–2009 period. Winter flows generally yielded the higher Ca/Sr values while the lower Ca/Sr values were typically associated with summer and spring melt samples.

3.5. Hydrogen and oxygen stable isotopes

Results from δD and $\delta^{18}O$ analyses (Fig. 8) can be used to identify the relative contributions differences in meteorological storm tracks. The range of $\delta^{18}O$ values in Chena River water samples is generally greater than the snow precipitation collected between 2005 and 2009 (-27.6 ± 5.3‰, n = 27) and lower than the rain samples collected from 2005 to 2009 (-16.6 ± 5.7‰, n = 19; T. Douglas, unpublished data). In general, spring melt river water has lower δD and $\delta^{18}O$ values due to the large fraction of snow melt water that makes up flow at this time, as has been observed for Yukon River waters (Guo and Macdonald, 2006; Guo et al., 2012). Samples collected during rain events tend to have higher δD and $\delta^{18}O$ values, especially in the 2005 samples that were collected immediately following the major rain event that ended a record dry period. The transition from late summer to fall recession and winter flows is generally associated with a decrease in δD and $\delta^{18}O$ values because these flows were associated with mean annual precipitation stable isotope signatures.

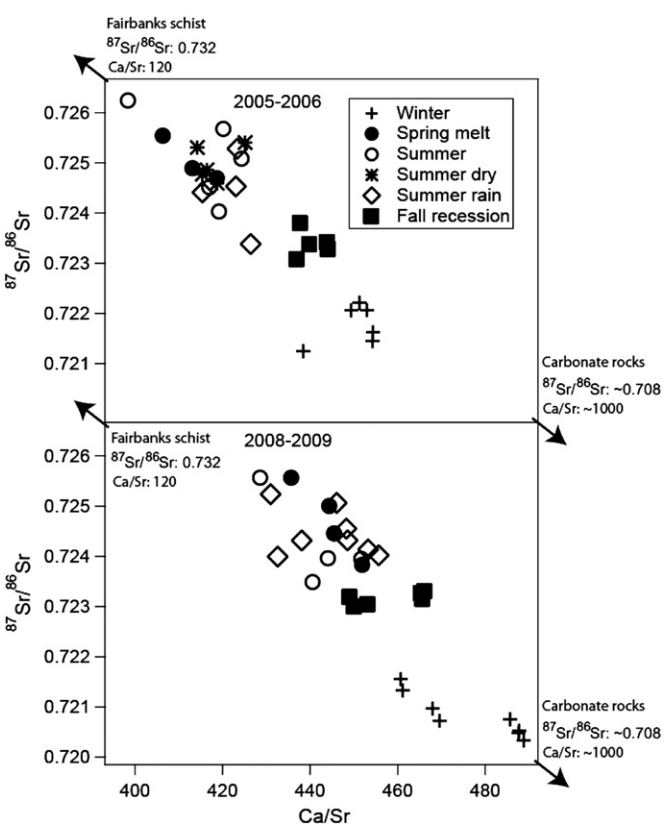

Fig. 7. $^{87}Sr/^{86}Sr$ versus Ca/Sr for the Chena River in 2005–2006 (upper panel) and 2008–2009 (lower panel).

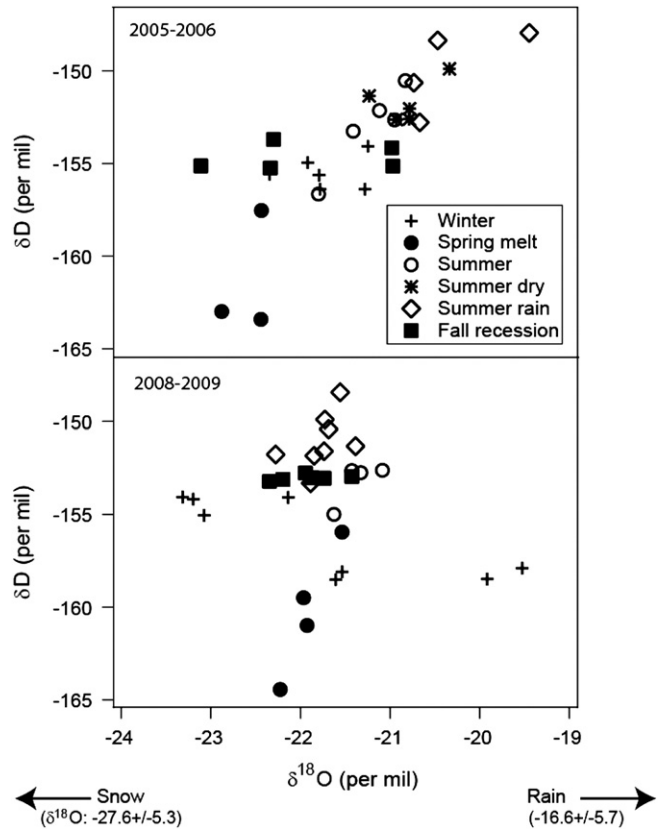

Fig. 8. Relationship between δD and $\delta^{18}O$ in the Chena River during 2005–2006 and 2008–2009. The range of snow and wet precipitation $\delta^{18}O$ values is also presented.

4. Discussion

4.1. Seasonality of nutrient dynamics

The seasonality of DOC and TDN concentrations in the Chena River are illustrated in Fig. 5. Similar to what was reported for the Chena River by Cai et al. (2008a) there is a strong correlation between discharge and DOC or TDN for our 2005–2006 and 2008–2009 samples. Events that led to increased discharge (like spring melt or summer rainstorms) were associated with the rapid flushing of DOC, TDN, and nitrate from surface soils (Fig. 5, Cai et al., 2008a,b). The very dry conditions during the summer of 2005 provided a unique opportunity for monitoring the fate of DOC, TDN, and nitrate during a period of extremely low discharge. All three of these carbon or nitrogen species decreased steadily with increasing time during the dry event. The large rain event in October that ended the dry period yielded elevated DOC, TDN, and nitrate concentrations in surface water. During winter seasons the river water TDN concentrations increased slightly in Chena River water. The source of this TDN was likely the degradation of dissolved organic nitrogen and the production of ammonia and nitrite as was suggested to explain similar patterns for the Yukon River (Guo and Macdonald, 2006; Guo et al., 2012).

Our measurements support results from previous studies showing that nutrient exports are rapidly flushed from surface soils during the large discharge events associated with snow melt runoff and during periods of major summer precipitation. Since elevated discharge is associated with increased nutrient concentrations, a large proportion of yearly nutrient fluxes from northern watersheds are attributable to these relatively short-lived flow events. This is consistent with results from previous studies of subarctic and arctic rivers (Striegl et al., 2005, 2007; Finlay et al., 2006; Raymond et al., 2007; Walvoord and Striegl, 2007; Cai et al., 2008b; McNamara et al., 2008; Frey and McClelland, 2009; Guo et al., 2012). The DOC mobilized during high

flow events is generally believed to be of modern age (Guo and Macdonald, 2006; Neff et al., 2006) and part of the DOC transported during spring melt may be labile (Holmes et al., 2008). As shown in Tables 1 and 3, not only did the concentrations of DOC and TDN vary with discharge, but the composition of organic matter in terms of its DOC/TDN ratio also showed a distinct difference between flow seasons, suggesting different DOM sources. Lower DOC/TDN ratios were observed during later fall and winter seasons, and higher DOC/TDN values were observed during spring melt and high stream flow seasons. It has been established at numerous Arctic and boreal biome watersheds that spring melt runoff is typically dominated by a large fraction of organic matter flushed from surface soils and vegetation (Laudon et al., 2004; Walvoord and Striegl, 2007; Holmes et al., 2012). As a consequence, we believe that flows through the Chena River watershed during the high flow spring melt season (and during some large summer rain storms associated with rapid, shallow flows) bring DOM mostly from surface soil and plant litter with high carbon but low nitrogen content. In contrast, in situ production during summer low flow conditions is believed to be contributed by freshly photosynthesized DOM, as suggested by the chlorophyll-a concentration (Cai et al., 2008a), resulting in lower DOC/TDN ratios.

Since snow melt occurs during the major seasonal change between winter and spring/summer any shift in the timing of snow melt would alter when the major nutrient flux occurs in northern watersheds. In northern Alaska the peak snow melt date has advanced 8 days since the 1960s (Stone et al., 2002). A similar shift in the Chena River may not alter the total flux of nutrients through the watershed during spring melt but an earlier snow melt would extend the growing season for soil microbes and vegetation that utilize nutrients. The biological response(s) to a longer growing season in the terrestrial Arctic and boreal zones could lead to major changes in soil (Fahnestock et al., 1998; Mikan et al., 2002; Edwards et al., 2006), vegetation (Flanagan et al., 2002; Walker et al., 2006; Høye et al., 2007) and aquatic (Hobbie et al., 1999; Sickman et al., 2003; Schindler and Smol, 2006; Frey and McClelland, 2009) ecosystem dynamics. These ecosystem changes, in turn, could provide feedbacks such as enhanced soil DOC export and subsequent carbon dioxide production and emission (Chapin et al., 2000; Davidson and Janssens, 2006; Field et al., 2007; Post et al., 2009).

4.2. Seasonality of watershed geochemistry

Major ion concentrations, $^{87}Sr/^{86}Sr$ and Ca/Sr ratios, and stable isotope ratios of hydrogen and oxygen provide widely utilized geochemical tracers for interpreting the mineral weathering sources and precipitation components in river waters. The major ion concentrations (excluding nitrate) and alkalinity values we measured in river water during both years were largely controlled by events that altered discharge and diluted flows, such as spring melt runoff or major rain events. We were able to identify some interesting trends by comparing the watershed geochemistry from similar flow regimes that occurred during both year-long sampling campaigns. First, the 2008 bicarbonate concentrations measured during late winter were almost twice the values measured in 2005 (Figs. 3 and 4) while the fall recession bicarbonate values in 2005 and 2008 were similar. Ca, Mg, and Na had roughly similar concentrations for both of the winter sampling periods and in both fall recession sampling periods, but the total cation and anion concentrations in microequivalents per Liter were roughly 20% higher in the late winter of 2008 than in the late winter of 2005. The reason for the elevated bicarbonate (and other major ion) values in the winter of 2008 is unclear, but they are most likely controlled by the previous year's late summer and fall recession period precipitation amounts and flow paths or ground water fluxes.

$^{87}Sr/^{86}Sr$ and Ca/Sr ratios provide information on cation sources to rivers without the confounding factor of dilution from rain and melt events or significant modification by ion exchange processes (i.e., Blum et al., 1998; Semhia et al., 2000; Hogan and Blum, 2003; Pett-Ridge et al., 2009; Keller et al., 2010). $^{87}Sr/^{86}Sr$ ratios are found to be at their annual minima and Ca/Sr ratios at their annual maxima during the winter base flow period. Spring melt and increased river discharge result in a large increase in $^{87}Sr/^{86}Sr$ and a decrease in Ca/Sr. $^{87}Sr/^{86}Sr$ remains high and Ca/Sr remains low throughout the summer period with continued correlation with discharge, and then the ratios gradually return to winter values during the fall. These ratios are thus strongly anti-correlated and provide insight into water flow paths and weathering reactions within the watershed that are controlled by geology and soil geochemistry.

The Chena River watershed is underlain largely by carbonaceous phyllites, calcareous phyllites, pelitic schists, and granitoids (Fig. 1). The phyllites and schists contain layers of massive carbonate as well as disseminated carbonate. Many previous studies have shown that when even a small proportion of the rock in a watershed contains carbonate, it can be an important factor controlling river water chemistry because carbonate minerals are so much more reactive with groundwater than silicate minerals (i.e., Blum et al., 1998; White et al., 1999; Jacobson et al., 2002). Because of the reactivity of carbonates they are usually depleted by weathering from the upper portions of soil profiles. Keller et al. (2007) found that calcium carbonate was depleted from near-surface soils developed on glacial deposits in the northern Brooks Range of Alaska. They found that the depth of carbonate depletion increased with the age of the glacial deposit, and thus the elapsed time of soil development. Soils estimated to be 50 to 120 ka old displayed carbonate depletion to a depth of about 1 m (Keller et al., 2007). Since the Chena River watershed was not glaciated during the Quaternary and the weathering surfaces are very old (certainly much older than 120 ka) we expect that carbonate is depleted to a depth of several meters to tens of meters as in other soils developed in non-glaciated areas.

It is our interpretation that changes in the $^{87}Sr/^{86}Sr$ and Ca/Sr ratios of the Chena River are an indication of seasonal differences in the interaction of ground water with carbonate versus silicate minerals. Carbonates associated with phyllites and pelitic schists are generally derived from marine limestones and thus have $^{87}Sr/^{86}Sr$ near 0.708 and Ca/Sr near 1000 (on a wt basis) (Veizer, 1989; Palmer and Edmond, 1992; Semhia et al., 2000). The silicate portions of the schists and phyllites are mica-rich and have high Rb/Sr ratios so they have high $^{87}Sr/^{86}Sr$ values. Silicate rocks also have much lower Ca/Sr ratios than carbonates. A study of $^{87}Sr/^{86}Sr$ in groundwater seeps in the Fairbanks schist had average $^{87}Sr/^{86}Sr$ and Ca/Sr ratios of 0.732 and 130, respectively (Goldfarb et al., 1997), which is a good estimate for the silicate weathering endmember in the Chena watershed. The linear array of $^{87}Sr/^{86}Sr$ and Ca/Sr ratios for Chena River water samples can be explained by mixing of Ca and Sr derived from the silicate endmember with Ca and Sr from the metamorphosed limestones in the watershed (Fig. 7).

During the winter base flow period surface soils freeze and groundwater flow is sourced from deep flow paths where carbonate minerals are generally present. As a consequence, the chemical signature shifts in the direction of carbonate. During spring, surface soils thaw and open shallow surface flow paths where soils are depleted in carbonate. This shifts the geochemical signature toward that of silicate. Mid-summer storm events are intermediate between these values because shallow flow paths are maintained but saturation of the soils causes discharge of some water traveling along deeper flow paths.

Another interesting watershed geochemical observation is the $^{87}Sr/^{86}Sr$ ratios measured during the extreme rain event that occurred in the summer of 2008. During both year-long sampling campaigns there was a strong seasonal relationship between $^{87}Sr/^{86}Sr$ values and discharge (Fig. 6), with samples collected during winter and fall recession (low discharge) varying in $^{87}Sr/^{86}Sr$ from 0.721

to 0.724 and 0.720 to 0.723, respectively, for 2005–2006 and 2008–2009. Samples collected during spring melt and summer (high discharge) were considerably higher and varied in $^{87}Sr/^{86}Sr$ from 0.724 to 0.726 and 0.723 to 0.725, respectively, for 2005–2006 and 2008–2009. During the extremely high flow periods measured between July 30th and August 14th, 2008 (>100 m^3/s), there is no obvious deviation in $^{87}Sr/^{86}Sr$ ratios correlated to discharge (Fig. 6). In most years the Chena River does not have discharge values greater than 150 m^3/s during spring melt or typical summer storms. The major storm in late 2008 produced flows greater than 250 m^3/s. This event also occurred late in the summer when deeper groundwater flow paths were already likely most dominant. Based on the $^{87}Sr/^{86}Sr$ ratios measured from these samples (Fig. 6), it is evident that the major precipitation event did not significantly perturb the balance of sources (i.e., carbonate versus silicate) being sampled by strontium isotopes during the summertime flow regime.

The stable hydrogen and oxygen isotopic composition of river water can be used to identify the relative contribution of wet precipitation, snow melt, and base flow water to the source of flow in the watershed (Fig. 8). There is a general trend of increasing δD with increasing $\delta^{18}O$ values, except for a unique situation with the 2008–2009 winter samples where increasing δD values are associated with decreasing $\delta^{18}O$ values. The winter season samples for 2008–2009 included waters collected during two different winter events: March and April 2008 and January, February, and March, 2009. The reason for the unexpected relationship between δD and $\delta^{18}O$ in these winter season samples is not clear but the timing of these anomalous samples may provide some insight. The two winter samples from the 2008–2009 sample campaign with the highest $\delta^{18}O$ values are from April 2008, immediately before the spring melt and their higher $\delta^{18}O$ values are indicative of a rain water source. The three winter samples from the 2008–2009 sample campaign with the lowest $\delta^{18}O$ values are from February and March, 2009 and their lower $\delta^{18}O$ values suggest a snow melt source. The stable isotope values for the rest of the seasonal samples are what would be expected given the meteoric water source of the river water (i.e. a generally positive relationship between δD and $\delta^{18}O$). The slope of the δD to $\delta^{18}O$ relationship is 3.3 in 2005–2006 and 3.9 in the 2008–2009 samples if the winter samples are not included.

By combining $^{87}Sr/^{86}Sr$ and stable oxygen isotope river water values with fields for snow and rain $\delta^{18}O$ and fields for shallow versus deep weathering $^{87}Sr/^{86}Sr$ signatures, the seasonality of flow paths and water sources can be explored together (Fig. 9). In both 2005–2006 and 2008–2009 the winter base flow had low $^{87}Sr/^{86}Sr$ values indicative of deep flow paths where carbonate is present. However, in the samples collected during the winter season of 2005–2006 there was a narrower range in $\delta^{18}O$ than in waters collected during the winter season of 2008–2009. Some of the variation in the 2008–2009 winter $\delta^{18}O$ values may be attributable to the different flow sources represented by the winter season samples. For example, the highest winter $\delta^{18}O$ values during the 2008–2009 year were measured from waters collected immediately prior to spring melt in mid to late April, 2008. These are the highest values measured for the entire year. The lowest winter $\delta^{18}O$ values for the 2008–2009 year were measured from water collected from February to March 2009. So these 2008–2009 "winter" samples actually represent flows from two different times during the 2008 and 2009 winter seasons. All of the winter season $^{87}Sr/^{86}Sr$ values are representative of deep flow paths while many of the winter $\delta^{18}O$ values are indicative of sources of water that are a mixture of snow and wet precipitation.

The 2005–2006 spring, summer and fall water samples exhibit a wider range in $\delta^{18}O$ values compared to 2008–2009. However, the $^{87}Sr/^{86}Sr$ values for the fall recession and spring melt are similar for the two different sampling years. Winter base flow, spring melt runoff and the fall recession seasons occur consistently every year in the watershed and these seasons are thus the most predictable. Changes in the timing of these seasons or their transitions may be associated with an alteration in river water biogeochemical characteristics. Whether a given summer experiences abnormally wet or dry periods or significant individual precipitation events is unpredictable and will remain so in the future.

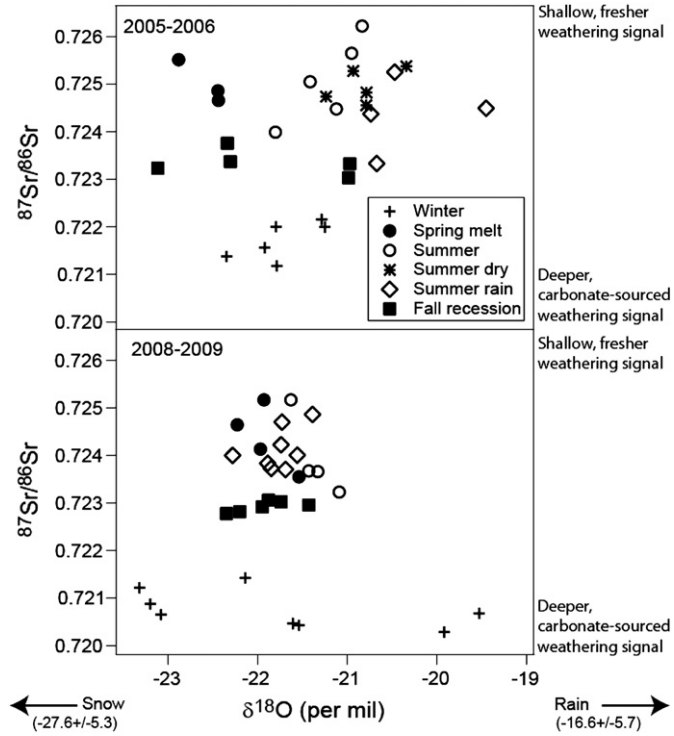

Fig. 9. $^{87}Sr/^{86}Sr$ versus $\delta^{18}O$ for the Chena River in 2005–2006 (upper panel) and 2008–2009 (lower panel). The range of snow and wet precipitation $\delta^{18}O$ values is also presented.

4.3. The potential effects of climate warming on permafrost and seasonality

It is expected that climate warming in Interior Alaska will cause extensive degradation of discontinuous permafrost (Osterkamp and Romanovsky, 1999; Marchenko et al., 2008). Since permafrost presents a confining region in the subsurface that constrains flow (Woo, 2000; Frey et al., 2007) it is likely that the loss of permafrost will alter subsurface flow and change ground water flow paths, the nature of water–rock interactions, and the export of carbon and other elements from watersheds. Any loss of permafrost that leads to changes in flow paths and water–rock interactions is expected to alter riverine nutrient (Cai et al., 2008a,b) and geochemical (Keller et al., 2007, 2010; Bagard et al., 2011) signatures.

Fig. 10 presents a schematic cross section of a hypothetical tributary watershed that illustrates the seasonality of flow regimes based on the results from this study. Since the Chena River watershed includes both areas underlain by permafrost and areas that are permafrost free we have simplified this spatial heterogeneity by presenting the permafrost as discrete bodies in the subsurface. In the winter season, during the lowest discharge of the year, the surface soils are frozen to ~1 m depth and the ground surface is covered by a blanket of snow. Flow to the river at this time is likely contributed from deep flow paths and the water biogeochemical signal is indicative of a greater extent of carbonate weathering. This season represents roughly half of the year. Future climate scenarios predict the shortening of this season as spring melt comes earlier and the summer to fall/winter transition arrives later.

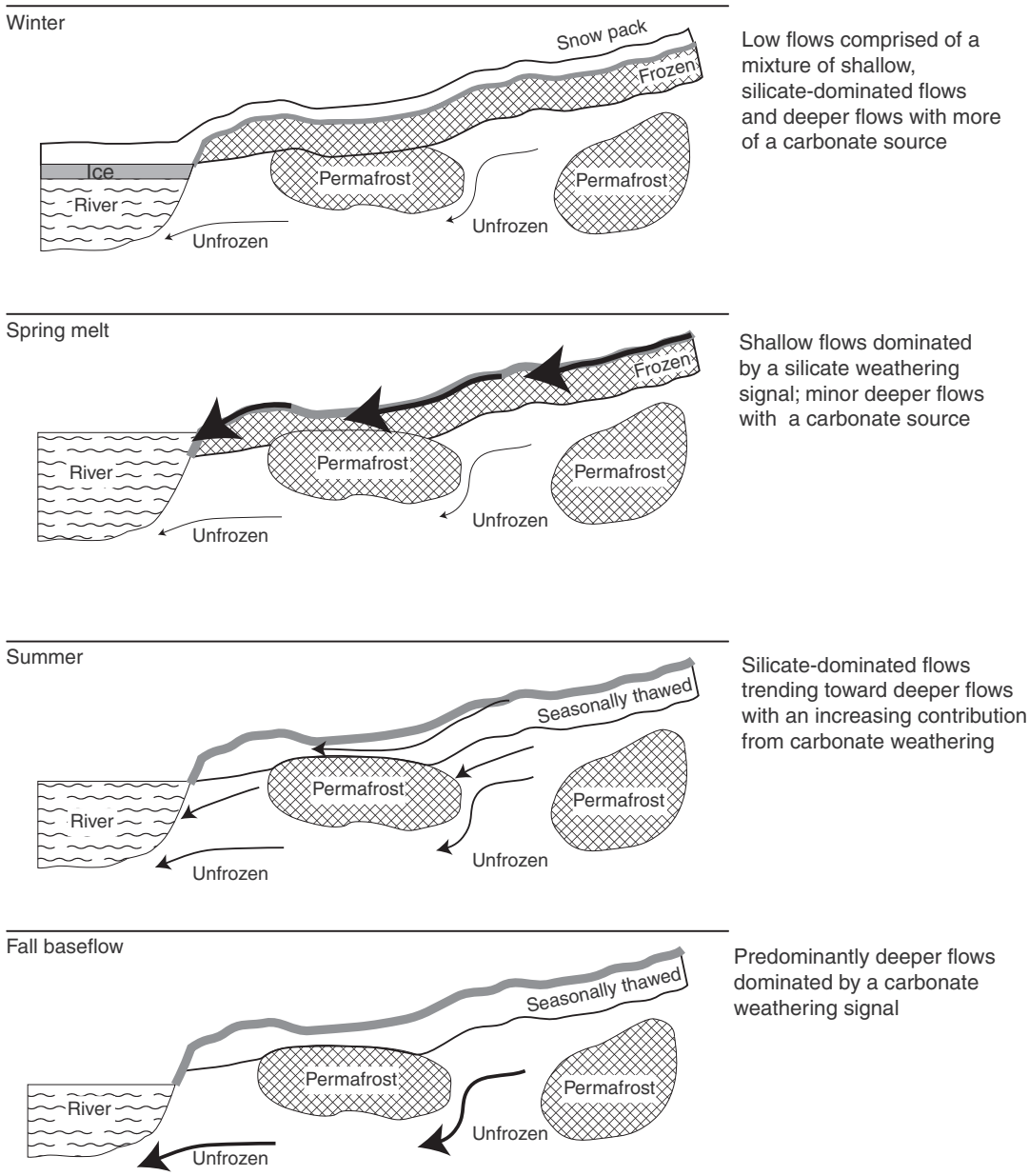

Fig. 10. A conceptual cross section through the Chena River illustrating the seasonality of flow regimes. The size of a given arrow is relative to the magnitude of flow from that path during a given season.

Spring melt represents the winter to spring transition and is the most dynamic seasonal event in northern watersheds (Guo et al., 2012). The typically highest yearly discharge rates bring elevated nutrient concentrations (and fluxes) downstream as surface soil and vegetation are flushed through shallow flow paths (MacLean et al., 1999). These shallow flows have a geochemical signature displaying a greater proportion of silicate weathering reactions and a general dilution of ground waters with the large influx of dilute snow melt water.

The summer season and its flow regimes are the most complicated, the least predictable, and likely the most difficult to integrate into predictive models for how climate warming will affect watershed biogeochemistry. Summers can experience extended wet or dry periods and major precipitation events, and these meteorologically driven impacts on river flow and biogeochemical characteristics are largely unpredictable.

In watersheds underlain by discontinuous permafrost the flow paths are channelized over, under, and around permafrost bodies due to their extremely low hydraulic conductivity. When taliks form, flows can be channelized over the top of the permafrost bodies. With increasing time after snow melt the seasonally thawed (active) layer expands downward. In a watershed with young carbonate-rich soils underlain by continuous permafrost the geochemical signal attributable to this thawing is associated with increasing input from carbonate weathering as the active layer thaws to greater depths (Keller et al., 2007, 2010). However, in watersheds with discontinuous permafrost and much older soils, the presence of deep flow paths that can contribute waters that have interacted with carbonate minerals at depth during the winter and shallower flow paths during the summer yields a smaller carbonate weathering signal as the summer progresses.

As a consequence of the complexity of flow paths, the measured and predicted wide scale thawing and degradation of permafrost in the discontinuous zone (Osterkamp and Romanovsky, 1999; Marchenko et al., 2008) may not be associated with an easily discernable watershed geochemical signal either seasonally or over decadal timescales. This is especially true for large river basins. The loss of

permafrost in watersheds underlain by discontinuous permafrost could lead to enhanced nutrient exports, especially if the active layer expands downward (O'Donnell and Jones, 2006; Petrone et al., 2006). However, wet precipitation provides the ultimate control on summer season nutrient and geochemical signatures. Extremely dry or wet periods are associated with unique biogeochemical signatures in the watershed and this complicates the potential to predict how watershed flows, biogeochemical signatures, or seasonal fluxes will respond to changing meteorology.

The other major seasonal transition, though arguably less identifiable than spring melt in terms of how it affects the river water biogeochemical signatures, is the transition from fall to winter. During this time the soil surface begins to freeze downward and flow paths become deeper and increasingly represent signatures indicative of carbonate weathering. The freezing front is initiated from cold surface temperatures and as it moves downward through the soil column it fractionates some soil water nutrients and solutes downward. The predicted movement of this seasonal transition to later in the year due to climate warming could lead to the presence of more surface soil and aquatic organic matter in watershed flows as the growing season expands later into the fall and the surface freeze-up and snowfall are delayed.

5. Conclusions

The results from this study show that northern rivers like the Chena can have a wide range in biogeochemical signatures that vary seasonally over the course of a year. Varied flow regimes are controlled by seasonality, precipitation, and the sources of river flows. As the seasons change from winter to spring the source of river waters is altered from low discharge deep flows with a carbonate weathering signal to high discharge surface flows with a more silicate-dominated weathering signal. Spring surface flows also carry a high organic matter content (DOC and TDN in this study). During the summer discharge is sourced from increasingly deeper flow paths that show a progressively greater carbonate weathering signal and a lower organic matter content. Permafrost provides a barrier to subsurface flow that likely leads to longer flow paths and enhanced water–rock interaction. Based on a conceptual model developed to explain seasonal differences in river water biogeochemistry, we infer that thawing of permafrost will lead to a decrease in the subsurface channelization of flows and changes in the timing and fluxes of organic matter and mineral weathering exports from northern watersheds.

It is apparent that the unique flow regimes and biogeochemical characteristics of subarctic rivers cannot be captured with sampling campaigns that are only active during single seasons or only represent unique events because of the wide variety in sources for river nutrient and geochemical fluxes and their varying biogeochemical signatures. Flow paths that contribute to subarctic rivers change over the course of the year, and so the effects of permafrost degradation on carbon and nutrient exports and biogeochemical signatures can only be identified through long term sampling programs that represent multiple flow regimes throughout the annual cycle.

Acknowledgments

We thank Yihua Cai, Mindy Juliana, Art Gelvin, and Laura Johnson for their assistance with field sampling. Zhengzhen Zhou helped with the DOC and TDN analysis. Amanda Barker commented on an earlier version of this manuscript. Two reviewers provided constructive comments that strengthened an earlier version of this manuscript and their efforts are greatly appreciated. Funding was provided by the U.S. Army Alaska Directorate of Public Works. Chris Hiemstra and Rainer Newberry helped us with development of the geologic map of the watershed.

References

Alaska Climate Research Center, 2011. http://climate.gi.alaska.edu/Climate/Location/Interior/Fairbanks.html (accessed December 19, 2011).

Bagard, M.-L., Chabaux, F., Pokrovsky, O.S., Viers, J., Prokushkin, A.S., Stille, P., Rihs, S., Schmitt, A.-D., Dupré, B., 2011. Seasonal variability of element fluxes in two Central Siberian rivers draining high latitude permafrost dominated areas. Geochimica et Cosmochimica Acta 71, 3335–3357.

Bense, V.F., Ferguson, G., Kooi, H., 2009. Evolution of shallow groundwater flow systems in areas of degrading permafrost. Geophysical Research Letters 36 (L22401). http://dx.doi.org/10.1029/2009GL039225 (6 pp.).

Blum, J.D., 1985. A petrologic and Rb–Sr isotopic study of intrusive rocks near Fairbanks, Alaska. Canadian Journal of Earth Sciences 22, 1314–1321.

Blum, J.D., Gazis, C.A., Jacobson, A., Chamberlain, C.P., 1998. Carbonate versus silicate weathering rates in the Raikot watershed within the high Himalayan crystalline series. Geology 26, 411–414.

Cai, Y., Guo, L., Douglas, T.A., 2008a. Temporal variations in organic carbon species and fluxes from the Chena River, Alaska. Limnology and Oceanography 53 (4), 1408–1419.

Cai, Y., Guo, L., Douglas, T.A., Whitledge, T.E., 2008b. Seasonal variations in nutrient concentrations and speciation in the Chena River, Alaska. Journal of Geophysical Research Biogeosciences 113 (G03035). http://dx.doi.org/10.1029/2008JG000733.

Carey, S.K., 2003. Dissolved organic carbon fluxes in a discontinuous permafrost subarctic alpine catchment Permafrost and Periglacial Processes 14 (2), 161–171.

Carey, S.K., Quinton, W.L., 2005. Evaluating runoff generation during summer using hydrometric, stable isotope and hydrochemical methods in a discontinuous permafrost alpine catchment. Hydrological Processes 19, 95–114.

Chapin, F.S., Mcguire, A.D., Randerson, J., Pielke, R., Baldocchi, D., Hobbie, S.E., Roulet, N., Eugster, W., Kasischke, E., Rastetter, E.B., Zimov, S.A., Running, S.W., 2000. Arctic and boreal ecosystems of western North America as components of the climate system. Global Change Biology 6, 211–223. http://dx.doi.org/10.1046/j.1365-2486.2000.06022.x.

Chapman, W.L., Walsh, J.E., 2007. Simulations of Arctic temperature and pressure by global coupled models. Journal of Climate 20 (4), 609–632.

Davidson, E.A., Janssens, I.A., 2006. Temperature sensitivity of soil carbon decomposition and feedbacks to climate change. Nature 440, 165–173. http://dx.doi.org/10.1038/nature04514.

Douglas, T.A., Layer, P.W., Newberry, R.N., Keskinen, M.J., 2002. Geochronologic and thermobarometric constraints on the metamorphic history of the Fairbanks Mining District, western Yukon–Tanana terrane, Alaska. Canadian Journal of Earth Sciences 39 (7), 1107–1126.

Douglas, T.A., Jorgenson, M.T., Kanevskiy, M.Z., Romanovsky, V.E., Shur, Y., Yoshikaw, K., 2008. Permafrost dynamics at the Fairbanks Permafrost Experimental Station near Fairbanks, Alaska. In: Kane, D.L., Hinkel, K.M. (Eds.), Proceedings of the Ninth International Conference on Permafrost. Institute of Northern Engineering University of Alaska Fairbanks, Fairbanks, Alaska, pp. 373–378.

Edwards, K.A., McCulloch, J., Kershaw, G.P., Jefferies, R.J., 2006. Soil microbial and nutrient dynamics in a wet Arctic sedge meadow in late winter and early spring. Soil Biology and Biochemistry 38 (9), 2843–2851.

Euskirchen, E.S., McGuire, A.D., Chapin III, F.S., Rupp, T.S., 2010. The changing effects of Alaska's boreal forests on the climate system. Canadian Journal of Forest Research 40, 1336–1346.

Fahnestock, J.T., Jones, M.H., Brooks, P.D., Walker, D.A., Welker, J.M., 1998. Winter and early spring CO_2 flux from tundra communities of northern Alaska. Journal of Geophysical Research 102 (D22), 29,925–29,931.

Field, C.B., Lobell, D.B., Peters, H.A., Chiarello, N.R., 2007. Feedbacks of terrestrial ecosystems to climate change. Annual Reviews in Environmental Resources 32, 1–29.

Finlay, J., Neff, J., Zimov, S., Davydova, A., Davydov, S., 2006. Snowmelt dominance of DOC in high-latitude watersheds: implications for characterization and flux of river DOC. Geophysical Research Letters 33, l10401.

Flanagan, L.B., Wever, L.A., Carlson, P.J., 2002. Seasonal and interannual variation in carbon dioxide exchange and carbon balance in a northern temperate grassland. Global Change Biology 8 (7), 599–615. http://dx.doi.org/10.1046/j.1365-2486.2002.00491.x.

Frey, K.E., McClelland, J.M., 2009. Impacts of permafrost degradation on arctic river biogeochemistry. Hydrological Processes 23 (1), 169–182.

Frey, K.E., Diegel, D.I., Smith, L.C., 2007. Geochemistry of west Siberian streams and their potential response to permafrost degradation. Water Resources Research 43 (W03406). http://dx.doi.org/10.1029/2006WR004902.

Goldfarb, R.J., Farmer, G.L., Cieutat, B.A., Meier, A.L., 1997. Major-element, trace-element, and strontium-isotope systematic of natural waters in the Fairbanks Mining District: constraints from local geology. U.S. Geological Survey Professional Paper 1614. (12 pp.).

Grosse, G., et al., 2011. Vulnerability of high-latitude soil organic carbon in North America to disturbance. Journal of Geophysical Research 116 (G00K06). http://dx.doi.org/10.1029/2010JG001507.

Guo, L., Macdonald, R.W., 2006. Source and transport of terrigenous organic matter in the upper Yukon River: evidence from isotope (^{13}C, ^{14}C and ^{15}N) composition of dissolved, colloidal and particulate phases. Global Biogeochemical Cycles 20, GB2011.

Guo, L., Ping, C.-L., Macdonald, R.W., 2007. Mobilization pathways of organic carbon from permafrost to arctic rivers in a changing climate. Geophysical Research Letters 34, L13603.

Guo, L., Cai, Y., Belzile, C., Macdonald, R., 2012. Sources and export fluxes of inorganic and organic carbon and nutrient species from the seasonally ice-covered Yukon River. Biogeochemistry 107, 187–206. http://dx.doi.org/10.1007/s10533-010-9545-z.

Hamilton, T.D., Ager, T.A., Robinson, S.W., 1983. Late Holocene ice wedges near Fairbanks, Alaska, U.S.A.: environmental setting and history of growth. Arctic and Alpine Research 15 (2), 157–168.

Hansen, V.L., Dusel-Bacon, C., 1998. Structural and kinematic evolution of the Yukon–Tanana terrane upland tectonites, east-central Alaska. A record of late Paleozoic to Mesozoic crustal assembly. Geological Society of America Bulletin 110 (2), 211–230.

Hinzman, L.D., Kane, D.L., Gieck, R.E., Everett, K.R., 1991. Hydrologic and thermal properties of the active layer in the Alaskan Arctic. Cold Regions Science and Technology 19 (2), 95–110.

Hinzman, L.D., Goering, D.J., Kane, D.L., 1998. A distributed thermal model for calculating temperature profiles and depth of thaw in permafrost regions. Journal of Geophysical Research 103 (D22), 28,975–28,991.

Hobbie, J.E., Peterson, B.J., Bettez, N., Deegan, L., O'Brien, W.J., Kling, G.W., Kipphut, G.W., Bowden, W.B., Hershey, A.E., 1999. Impact of global change on the biogeochemistry and ecology of an Arctic freshwater system. Polar Research 18, 207–214. http://dx.doi.org/10.1111/j.1751-8369.1999.tb00295.x.

Hogan, J.F., Blum, J.D., 2003. Strontium isotopes as a tracer of hydrologic flowpaths in a small forested catchment. Water Resources Research 39, 1282–1294. http://dx.doi.org/10.1029/2002WR001856.

Holmes, R.M., McClelland, J.W., Raymond, P.A., Frazer, B.B., Peterson, B.J., Stieglitz, M., 2008. Lability of DOC transported by Alaskan rivers to the Arctic Ocean. Geophysical Research Letters 35, L03402. http://dx.doi.org/10.1029/2007GL032837.

Holmes, R.M., McClelland, J.W., Peterson, B.J., Tank, S.E., Bulygina, E., Eglinton, T.I., Gordeev, V.V., Gurtovaya, T.Y., Raymond, P.A., Repeta, D.J., Staples, R., Striegl, R.G., Zhulidov, A.V., Zimov, S.A., 2012. Seasonal and annual fluxes of nutrients and organic matter from large rivers to the Arctic Ocean and surrounding seas. Estuaries and Coasts 35, 369–382. http://dx.doi.org/10.1007/s12237-011-9386-6.

Høye, T.T., Post, E., Meltofte, H., Schmidt, N.M., Forchhammer, M.C., 2007. Rapid advancement of spring in the high Arctic. Current Biology 17 (12), R449–R451. http://dx.doi.org/10.1016/j.cub.2007.04.047.

Jacobson, A.D., Blum, J.D., Walter, L.M., 2002. A carbonate equilibria approach to reconciling the elemental and Sr isotopic geochemistry of Himalayan stream waters. Geochimica et Cosmochimica Acta 66, 3417–3429.

Johnstone, J.F., Hollingsworth, T.N., Chapin III, F.S., Mack, M.C., 2010. Changes in fire regime break the legacy lock on successional trajectories in Alaskan boreal forest. Global Change Biology 16, 1281–1295. http://dx.doi.org/10.1111/j.1365-2486.2009.02051.x.

Jorgenson, M.T., Racine, C.H., Walters, J.C., Osterkamp, T.E., 2001. Permafrost degradation and ecological changes associated with a warming climate in central Alaska. Climatic Change 48, 551–579.

Jorgenson, M.T., Shur, Y.L., Pullman, E.R., 2006. Abrupt increases in permafrost degradation in Arctic Alaska. Geophysical Research Letters 33, L02503.

Kane, D.L., Hinzman, L.D., Zarling, J.P., 1991. Thermal response of the active layer to climatic warming in a permafrost environment. Cold Regions Science and Technology 19 (2), 111–122.

Karlstrom, N.V., Coulter, H.W., Fernald, A.T., Williams, J.R., Hopkins, D.M., Péwé, T.L., Drewes, J.R., Muller, E.R., Condon, W.H., 1964. Surficial geology of Alaska. U.S. Geological Survey Miscellaneous Geological Investigations, Map, pp. 1–357.

Kauman, D.S., Manley, W.F., 2004. Pleistocene maximum and Late Wisconsinan glacier extents across Alaska, U.S.A. Developments in Quaternary Sciences 2 (Part B), 9–27.

Keller, K., Blum, J.D., Kling, G.W., 2007. Geochemistry of soils and streams on surfaces of varying ages in Arctic Alaska. Arctic, Antarctic, and Alpine Research 39, 84–98.

Keller, K., Blum, J.D., Kling, G.W., 2010. Stream geochemistry as an indicator of increasing permafrost thaw depth in an arctic watershed. Chemical Geology 273 (1–2), 76–81.

Laudon, H., Köhler, S., Buffam, I., 2004. Seasonal TOC export from seven boreal catchments in northern Sweden. Aquatic Sciences 66, 223–230. http://dx.doi.org/10.1007/s00027-004-0700-2.

MacLean, R., Oswood, M.W., Irons III, J.G., McDowell, W.H., 1999. The effect of permafrost on stream biogeochemistry: a case study of two streams in the Alaskan (U.S.A.) taiga. Biogeochemistry 47, 239–267.

Marchenko, S., Romanovsky, V., Tipenko, G., 2008. Numerical modeling of spatial permafrost dynamics in Alaska. In: Kane, D.L., Hinkel, K.M. (Eds.), Proceedings of the Ninth International Conference on Permafrost. Institute of Northern Engineering University of Alaska Fairbanks, Fairbanks, Alaska, pp. 1125–1130.

McGuire, A.D., Anderson, L.G., Christensen, T.R., Dallimore, S., Guo, L., Hayes, D.L., Heimann, M., Lorenson, T.D., Macdonald, R.W., Roulet, N., 2009. Sensitivity of the carbon cycles in the Arctic to climate change. Ecological Monographs 79 (4), 523–555.

McNamara, J., Kane, D., Hobbie, J., Kling, G.W., 2008. Hydrologic and biogeochemical controls on the spatial and temporal patterns of nitrogen and phosphorus in the Kuparuk River, Arctic Alaska. Hydrological Processes 22, 3294–3309. http://dx.doi.org/10.1002/hyp.6920.

Mikan, C.J., Schimel, J.P., Doyle, A.P., 2002. Temperature controls of microbial respiration in arctic tundra soils above and below freezing. Soil Biology and Biochemistry 34 (11), 1785–1795.

Neff, J., Finlay, J., Zimov, S., Davydov, S., Carrasco, J., Schuur, E., Davydova, A., 2006. Seasonal changes in the age and structure of dissolved organic carbon in Siberian rivers and streams. Geophysical Research Letters 33 (23), L23401.

Newberry, R.J., Bundtzen, T.K., Clautice, K.H., Combellick, R.A., Douglas, T.A., Laird, G.M., Liss, S.A., Pinney, D.S., Reifenstuhl, R.R., Solie, D.N., 1996. Preliminary geologic map of the Fairbanks Mining District, Alaska. Alaska Division of Geological and Geophysical Surveys Public Data File 96–16, 17 p., 2 sheets, scale 1:63,360.

O'Donnell, J.A., Jones Jr., J.B., 2006. Nitrogen retention in the riparian zone of catchments underlain by discontinuous permafrost. Freshwater Biology 51, 854–864.

Osterkamp, T.E., 2007. Characteristics of the recent warming of permafrost in Alaska. Journal of Geophysical Research 112, F02S02. http://dx.doi.org/10.1029/2006JF000578.

Osterkamp, T.E., Jorgenson, J.C., 2006. Warming of permafrost in the Arctic National Wildlife Refuge, Alaska. Permafrost and Periglacial Processes 17, 65–69. http://dx.doi.org/10.1002/ppp. 538.

Osterkamp, T.E., Romanovsky, V.E., 1999. Evidence for warming and thawing of discontinuous permafrost in Alaska. Permafrost and Periglacial Processes 10, 17–37.

Osterkamp, T.E., Vierick, L., Shur, Y., Jorgenson, M.T., Racine, C., Doyle, A., Boone, R.D., 2000. Observations of thermokarst and its impact on boreal forests in Alaska, U.S.A. Arctic, Antarctic, and Alpine Research 32 (3), 303–315.

Palmer, M.R., Edmond, J.M., 1992. Controls over the strontium isotope composition of river water. Geochimica et Cosmochimica Acta 56 (5), 2099–2111.

Petrone, K.C., Jones, J.B., Hinzman, L.D., Boone, R.D., 2006. Seasonal export of carbon, nitrogen, and major solutes from Alaskan catchments with discontinuous permafrost. Journal of Geophysical Research 111, G02020.

Pett-Ridge, J.C., Derry, L.A., Barrows, J.K., 2009. Ca/Sr and 87Sr/86Sr ratios as tracers of Ca and Sr cycling in the Rio Icacos watershed, Luquillo Mountains, Puerto Rico. Chemical Geology 267, 32–45.

Post, E., et al., 2009. Ecological dynamics across the Arctic associated with recent climate change. Science 325, 1355–1358. http://dx.doi.org/10.1126/science.1173113.

Racine, C.H., Walters, J.C., 1994. Groundwater-discharge fens in the Tanana Lowlands, Interior Alaska, U.S.A. Arctic and Alpine Research 26 (4), 418–426.

Raymond, P.A., McClelland, J., Holmes, R., Zhulidov, A., Mull, K., Peterson, B., Striegl, R., Aiken, G., Gurtovaya, T., 2007. Flux and age of dissolved organic carbon exported to the Arctic Ocean: a carbon isotopic study of the five largest arctic rivers. Global Biogeochemical Cycles 21 (4), 1–B4011.

Rember, R.D., Trefry, J.H., 2004. Increased concentrations of dissolved trace metals and organic carbon during snowmelt in rivers of the Alaskan Arctic. Geochimica et Cosmochimica Acta 68 (3), 477–489.

Schindler, D.W., Smol, J.P., 2006. Cumulative effects of climate warming and other human activities on freshwaters of Arctic and Subarctic North America. AMBIO: A Journal of the Human Environment 35 (4), 160–168.

Semhia, K., Clauer, N., Probst, J.L., 2000. Strontium isotope compositions of river waters as records of lithology-dependent mass transfers: the Garonne River and its tributaries (SW France). Chemical Geology 168 (3–4), 173–193.

Shur, Y.L., Jorgenson, M.T., 2007. Patterns of permafrost formation and degradation in relation to climate and ecosystems. Permafrost and Periglacial Processes 18, 7–19.

Sickman, J.O., Leydecker, A., Chang, C.Y., Kendall, C., Melack, J.M., Lucero, D.M., Schimel, J., 2003. Mechanisms underlying export of N from high-elevation catchments during seasonal transitions. Biogeochemistry 64 (1), 1–24. http://dx.doi.org/10.1023/A:1024928317057.

Sierra, C.A., Harmon, M.E., Thomann, E., Perakis, S.S., Loescher, H.W., 2011. Amplification and dampening of soil respiration by changes in temperature variability. Biogeosciences 8, 951–961.

Stolpe, B., Guo, L., Shiller, A.M., Aiken, G.R., in press. Abundance, size distributions and trace-element binding of organic and iron-rich nanocolloids in Alaskan rivers as revealed by flow field flow fractionation and ICP-MS. Geochimica et Cosmochimica Acta.

Stone, R.S., Dutton, E.S., Harris, J.M., Longenecker, D., 2002. Earlier spring snowmelt in northern Alaska as an indicator of climate change. Journal of Geophysical Research 107 (4089). http://dx.doi.org/10.1029/2000JD000286.

Striegl, R.G., Aiken, G.R., Dornblaser, M.M., Raymond, P.A., Wickland, K.P., 2005. A decrease in discharge-normalized DOC export by the Yukon River during summer through autumn. Geophysical Research Letters 32 (L21413). http://dx.doi.org/10.1029/2005GL024413.

Striegl, R.G., Dornblaser, M.M., Aiken, G.R., Wickland, K.P., Raymond, P.A., 2007. Carbon export and cycling by the Yukon, Tanana, and Porcupine rivers, Alaska, 2001–2005. Water Resources Research 43, W02411. http://dx.doi.org/10D1029/2006WR005201.

Stumm, W., Morgan, J.J., 1996. Aquatic Chemistry: Chemical Equilibria and Rates in Natural Waters, 3rd ed. Wiley-Intersci, Hoboken, N. J . (1040 pp.).

Tarnocai, C., Canadell, J.G., Schuur, E.A.G., Kuhry, P., Mazhitova, G., Zimov, S., 2009. Soil organic carbon pools in the northern circumpolar permafrost. Global Biogeochemical Cycles 23, GB2023. http://dx.doi.org/10.1029/2008GB003327.

Thompson, D.K., Woo, M.-K., 2009. Seasonal hydrochemistry of a high Arctic wetland complex. Hydrological Processes 23, 1397–1407. http://dx.doi.org/10.1002/hyp.7271.

Veizer, J., 1989. Strontium isotopes in seawater through time. Annual Reviews in Earth and Planetary Science 17, 141–167.

Walker, M.D., Wahren, C.H., Hollister, R.D., Henry, G.H.R., Ahlquist, L.E., et al., 2006. Plant community responses to experimental warming across the tundra biome. Proceedings of the National Academy of Sciences of the United States of America 103, 1342–1346.

Walvoord, M., Striegl, R.G., 2007. Increased groundwater to stream discharge from permafrost thawing in the Yukon River Basin: potential impacts on lateral export of carbon and nitrogen. Geophysical Research Letters 34 (L12402). http://dx.doi.org/10.1029/2007GL030216.

Wendler, G., Conner, J., Moore, B., Shulski, M., Stuefer, M., 2010. Climatology of Alaskan wildfires with special emphasis on the extreme year of 2004. Theoretical and Applied Climatology. http://dx.doi.org/10.1007/s00704-010-0357-9.

White, A.F., Bullen, T., Davison, D., Vivit, V., Schulz, M.S., Clow, D.W., 1999. The role of disseminated calcite in the chemical weathering of granitoid rocks. Geochimica et Cosmochimica Acta 63 (13–14), 1939–1953.

Wilson, F.H., Dover, J.H., Bradley, D.C., Weber, F.R., Bundtzen, T.K., Haeussler, P.J., 1998. Geologic map of Central (Interior) Alaska. U.S. Geological Survey Open-File Report OF 98-133. (86 pp.).

Wolken, J.M., Hollingsworth, T.N., Rupp, T.S., Chapin III, F.S., Trainor, S.F., Barrett, T.M., Sullivan, P.F., McGuire, A.D., Euskirchen, E.S., Hennon, P.E., Beever, E.A., Conn, J.S., Crone, L.K., D'Amore, D.V., Fresco, N., Hanley, T.A., Kielland, K., Kruse, J.J., Patterson, T., Schuur, E.A.G., Verbyla, D.L., Yarie, J., 2011. Evidence and implications of recent and projected climate change in Alaska's forest ecosystems. Ecosphere 2 (11), 1–35.

Woo, M.K., 2000. Permafrost and hydrology. The Arctic: Environment, People, Policy, pp. 57–96.

Zhou, Z., Guo, L., 2012. Evolution of the optical properties of seawater influenced by the DWH oil spill in the Gulf of Mexico. Environmental Research Letters 7, 025301. http://dx.doi.org/10.1088/1748-9326/7/2/025301.

Zimov, S.A., Schuur, E.A.G., Chapin, F.S.I.I.I., 2006a. Permafrost and the global carbon budget. Science 312, 1612–1613.

Zimov, S.A., Davydov, S.P., Zimova, G.M., Davydova, A.I., Schuur, E.A.G., Dutta, K., Chapin III, F.S., 2006b. Permafrost carbon: stock and decomposability of a globally significant carbon pool. Geophysical Research Letters 33, L20502. http://dx.doi.org/10.1029/2006GL027484.